

ASYNCHRONOUS OPERATION OF
A.C. GENERATORS WITH AND
WITHOUT RECTIFIER IN FIELD CIRCUIT

By:

ROBERT ALEXANDER HANNA

A dissertation submitted for
the degree of Master of Science
of the University of London.

Queen Mary College,
Electrical Engineering Dept.,
Mile End Road,
London E. 1.

December, 1973.

ABSTRACT

Many modern large a.c. generators are designed with brushless excitation systems mainly for reasons of advantages gained in maintenance and reliability. In such schemes the excitation power is derived from an a.c. generator through a rectifier bridge mounted on the rotating shaft. If such generator loses synchronism and slips with respect to the power network, the field current which will be induced in this condition cannot reverse and the rectifier cells will be subjected to large inverse voltages.

This situation has been studied experimentally and theoretically in this project in relation to a 69 kVA laboratory a.c. generator with rectifier in its field circuit.

Asynchronous operation during all tests was imposed by sudden removal of the excitation supply for the machine, which initially was carrying fractional steady load.

For comparison with the brushless machines, loss of synchronism was also investigated experimentally for conventional excitation system, when the field winding is left open or closed through a discharge resistor. This comparison concentrates on the behaviour of induced field voltage and current,

slip and armature current following the above disturbance.

For the case of an a.c. generator with rectifier in the field circuit, the test programme was further extended to investigate the effect of damping winding and the presence of discharge resistor on the induced inverse voltage and field current.

Theoretically, the performance of an a.c. generator with only a rectifier in the field circuit during asynchronous operation was studied using the method of analysis developed by Rao and MacDonald. However, some modifications were found necessary in the formulation of the field circuit equations to suit the approach of this work. The method of analysis used was quite general, capable of predicting both the transient condition prevailing immediately after the disturbance as well as the state eventually reached by the machine, in which the slip was cyclically varying. This implies non-linear performance equations which have to be solved iteratively by a digital computer. The prediction and test results were found to be in agreement quite reasonably for practical purposes.

ACKNOWLEDGEMENTS

I wish to express my sincere gratitude to my Supervisor, Mr. A. Twardzicki of Queen Mary College, for his invaluable help and assistance in the preparation and completion of this project.

I also wish to thank Dr. D.C. MacDonald of Imperial College for his continual interest in the work.

I am grateful to the Ministry of Higher Education and Scientific Research of the Government of the Republic of Iraq for their generous financial support which made this work possible.

Finally, I wish to thank the technicians for their indispensable contribution in the laboratory work, and also Shelagh for typing the manuscript.

To:

My beloved parents

LIST OF SYMBOLS

The symbols repeatedly used are listed below. Other symbols are explained in the text.

Unless otherwise stated, all quantities are expressed in per unit in accordance with reference 9. In general, varying quantities are denoted by small letters.

v_d, v_q	:	d - and q-axis voltages
i_d, i_q	:	d - and q-axis currents
v_f	:	field voltage induced in the field winding under asynchronous operation.
i_f	:	field current
r_a, r_f, r_{kd}, r_{kq}	:	resistance of the armature, field and damper winding.
$L_f = L_{md} + l_f$)		
$L_d = L_{md} + l_a$)		complete self-inductances of
$L_q = L_{mq} + l_a$)	:	the field, d-axis, q-axis and
$L_{kd} = L_{md} + l_{kd}$)		damper circuit
$L_{kq} = L_{mq} + l_{kq}$)		
x_f, x_a, x_{kd}, x_{kq})	:	leakage reactances and inductances
	:	of the field, armature and damper
l_f, l_a, l_{kd}, l_{kq})		winding
x_{md}, x_{mq})	:	magnetizing reactances and inductance
L_{md}, L_{mq})	:	of the armature along d- and q-axis

$\psi_d, \psi_q, \psi_f, \psi_{kd}, \psi_{kq}$:	flux linkages
T_e	:	electromagnetic torque
P, Q	:	active and reactive power at the generator terminal.
δ	:	rotor angle of the generator with respect to the infinite bus
ω, ω_o	:	actual and synchronous speed in rad/S.
s	:	Slip
H	:	^{inertia} inertia constant
f	:	supply frequency, Hz.
T	:	time constant
p	:	operator $\frac{d}{dt}$

CONTENTS

	<u>Page</u>
Abstract	I
Acknowledgements	III
List of Symbols	V
CHAPTER 1 INTRODUCTION	1
1.1 Excitation schemes for a.c. synchronous generators	1
1.2 Currents and voltages induced in excitation circuits	6
1.3 Fault conditions in brushless a.c. generators	8
1.4 Scope of the project	9
CHAPTER 2 THEORETICAL ANALYSIS OF ASYNCHRONOUS OPERATION WITH RECTIFIER IN FIELD CIRCUIT	12
2.1 Introduction	12
2.2 General machine equations	13
2.3 Formulation of performance equations for asynchronous operation	19
2.4 Step-by-step solution of machine equations	23
2.5 Solution of performance equations using a digital computer	24
2.6 Comments	27
CHAPTER 3 EXPERIMENTAL INVESTIGATION OF A.C. GENERATOR WITH AND WITHOUT RECTIFIER IN FIELD CIRCUIT	28
3.1 Introduction	28
3.2 Particulars of a.c. generator and associated equipment	29

3.3	Preliminary experimental work	31
3.4	Test instrumentation and recording equipment	33
3.5	Programme of tests and results	37
3.5.1	Field winding open	38
3.5.2	Field winding closed through a protective resistor	41
3.5.3	Field winding closed through a rectifier	43
3.5.4	Rectifier shunted by a protective resistor across the field winding	47
3.5.5	Effects of modifying damping winding	48
CHAPTER 4	DISCUSSION AND CONCLUSIONS	62
4.1	Comparison between tested and computed performance	62
4.2	Conclusions	67
4.3	Suggestions for further work	72
TABLES		74
APPENDICES		76
REFERENCES		83

CHAPTER 1

INTRODUCTION

1.1 EXCITATION SCHEMES FOR A.C. SYNCHRONOUS GENERATORS

The progress that has been made over recent years in the design and manufacture of a.c. generators has resulted in considerably larger power output from machines of given size.

These large output ratings entail also larger excitation power requirements. In conventional schemes, the excitation power for generators rated up to about 60 MW¹ was provided by directly coupled d.c. exciters. For larger ratings up to about 275 MW¹ low speed d.c. exciters, gear-driven from the generator shaft, were used.

The configuration of field winding in high speed a.c. generators and the relatively low voltages for which d.c. machines can be designed, means that the increase of excitation power is achieved mainly by raising the generator field current. Typical example² is exciter of rating 2200 kW for a 500 MW generator. The nominal voltage of such exciter is usually in the range of 375-500V with current rating of up to 4500 A.

The current handling capacity of d.c. exciters, direct coupled to turbo-generator, is limited by the maximum current densities in commutator and its brushgear owing to commutation difficulties; moreover, large number of brushes is needed on the rings and commutators to transfer the current between stationary and rotating circuit, and this increases the task of maintenance.

Use of geared exciters, running at lower speed, helped only in some respects, but obviously resulted in larger size of exciters, which increase the capital cost of the plant³.

These problems with conventional d.c. exciters stimulated the development of alternative sources of excitation power. Initially, schemes were proposed in which excitation power was derived in one of the following ways⁴:

- a) From auxiliary a.c. power network.
- b) From the terminals of the a.c. generator itself.
- c) From an a.c. exciter mounted on the shaft of the main machine.

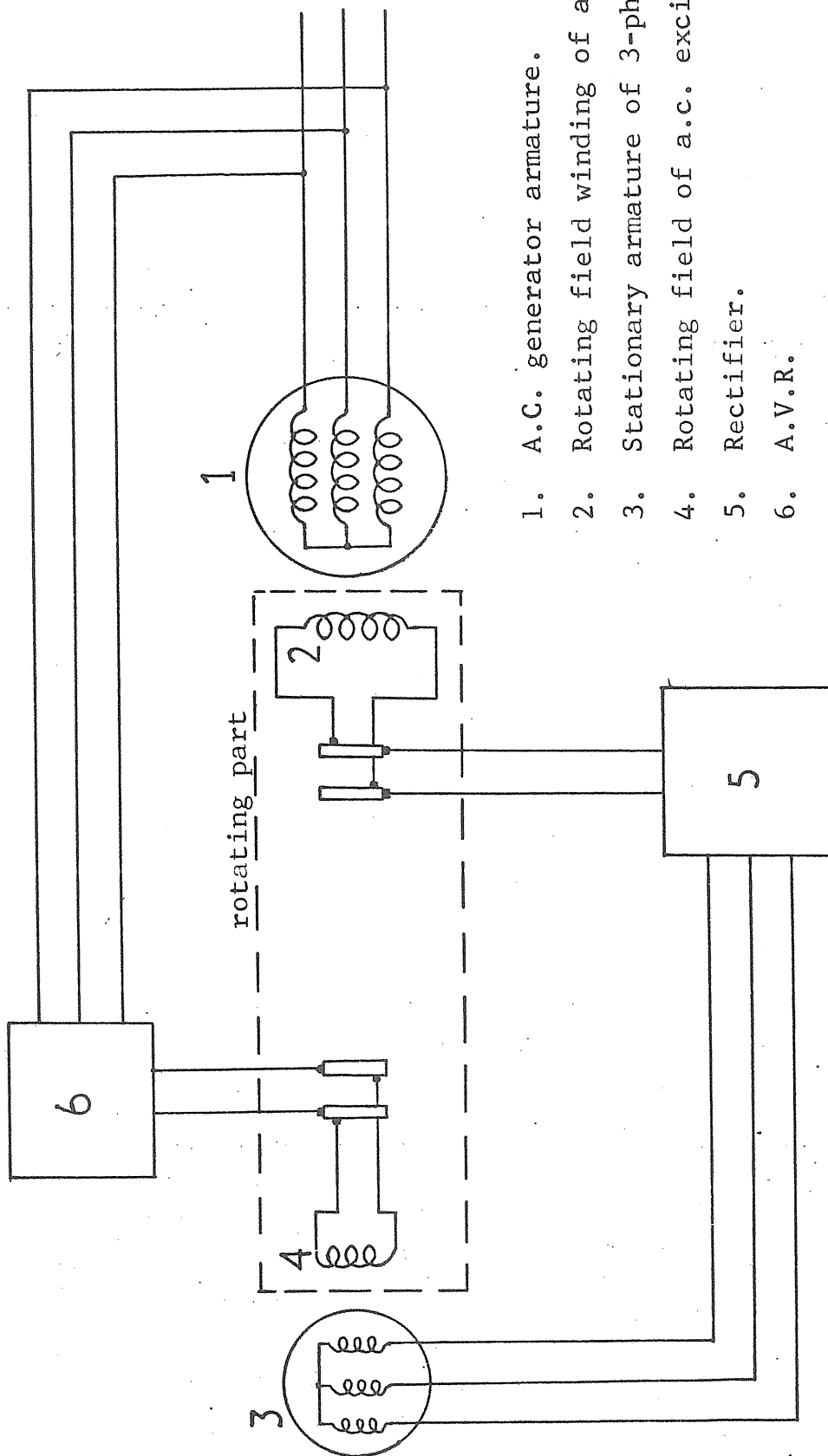
In either of the above schemes the a.c. excitation power was rectified by mercury arc rectifier, ignitrons or ionic valves.

Such schemes were bulky, needed considerable auxiliary equipment and specialised maintenance. None of these schemes were ever widely used as an alternative to the rotary d.c. exciters.

Eventually, schemes using a.c. exciters in conjunction with static semi-conductor rectifiers⁵ were used to replace the d.c. exciter. Initially, germanium rectifiers were used for this purpose, but development of more reliable silicon semi-conductor rectifier of lower efficiency than germanium one but of much higher current, voltage and temperature capability, has greatly accelerated progress in the design of rectifier excitation systems for large powers.

The armature of such a.c. exciters used with static rectifiers is stationary as shown in Fig. 1.1; the commutator with its brushgear and speed-reducing gear are dispensed with.

Although such a scheme obviates the problems associated with commutation and brushgear and presents no difficulties for large rating or high speed turbo-generators, it does not solve the problems of current collection at the rotor slip-rings. Attention was therefore directed towards the "brushless" scheme as shown in Fig. 1.2. Here, the rectifier is rotating and is mounted on the same shaft as the field of the a.c. generator;



1. A.C. generator armature.
2. Rotating field winding of a.c. generator.
3. Stationary armature of 3-ph exciter.
4. Rotating field of a.c. exciter.
5. Rectifier.
6. A.V.R.

Fig. 1.1 Excitation system with a.c. exciter and static rectifier.

1. Main a.c. generator armature.
2. Rotating field winding of main generator.
3. Rotating armature of 3-ph a.c. exciter.
4. Stationary field of a.c. exciter.
5. Pilot exciter armature.
6. Permanent magnet rotor of pilot exciter.
7. A.V.R.
8. Transformer.
9. Rotating bridge rectifier.

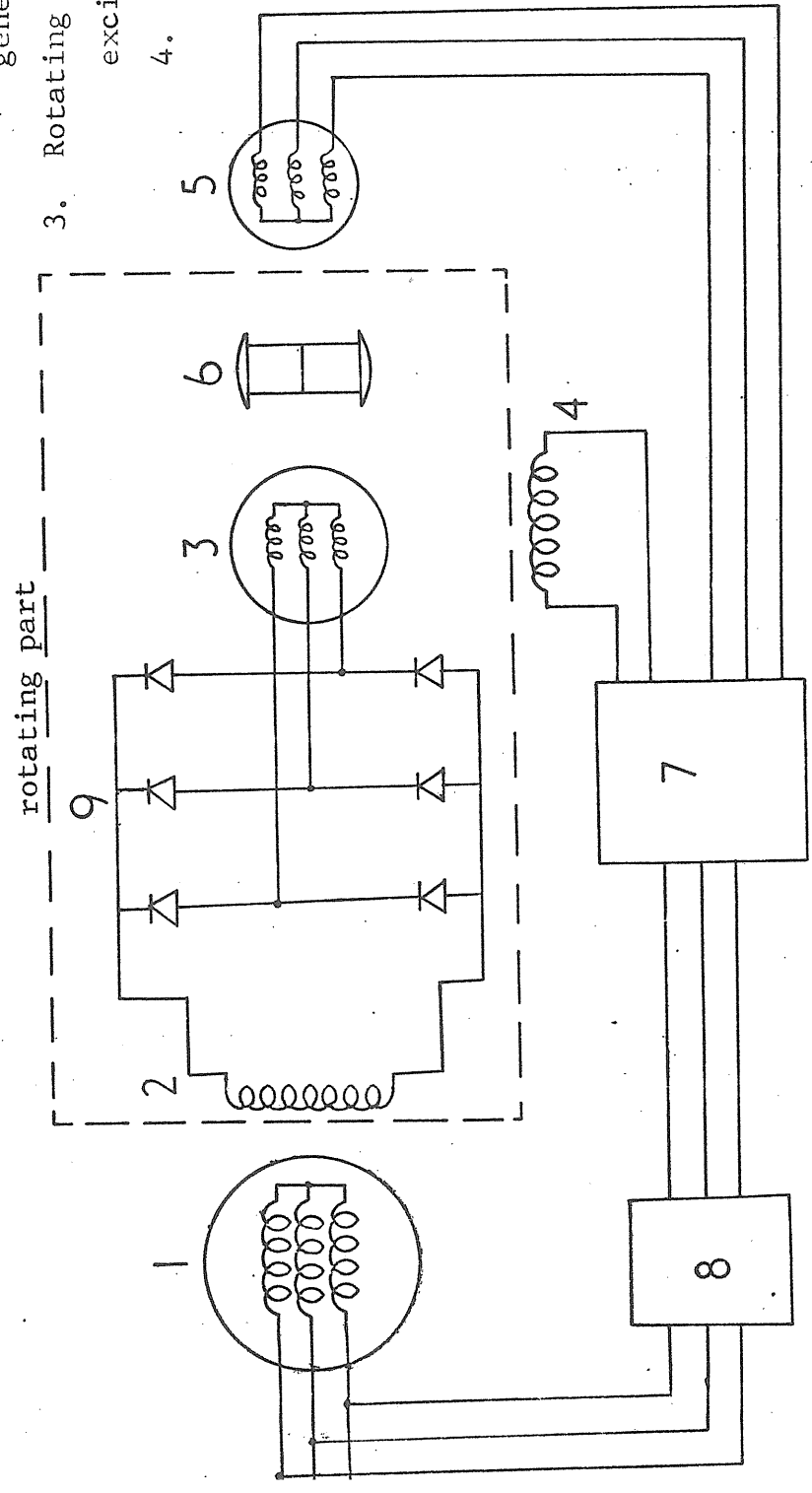


Fig. 1.2 Outline of a brushless excitation system.

the rectifier is fed from a.c. exciter with a rotating armature and stationary field. The total excitation power requirement, including the power supply of the regulator, is derived from the generator shaft.

The relatively novel excitation system functions as follows:

The small permanent magnetic pilot exciter stator furnishes excitation power to the regulator system, which in turn energizes the stationary field of main a.c. exciter. The output of the a.c. exciter rotating armature is fed through shaft mounted rectifier into the field winding of the a.c. generator. Hence, all sliding contacts are eliminated, which is clearly desirable from the point of view of reliability and reduce maintenance.

1.2 CURRENTS AND VOLTAGES INDUCED IN EXCITATION CIRCUITS

One of the most important problems arising in the new scheme is to predict and limit the current and voltage induced in the field circuit under some extreme load condition or during abnormal operating conditions associated with faults in the power network to which the a.c. generator is connected or in excitation circuit itself. If proper allowance has not been

made, such faults could result either in excessive currents in the diodes themselves or high reverse voltages across them, with the possibility of their damage or failure.

Since in the forward or conducting direction the rectifier provides a low impedance path comparable with that of the circuit through the armature of a d.c. exciter, the behaviour of brushless machine, during faults where the field current is always in the forward direction, is similar to that of machines with conventional excitation. But if the field current attempts to reverse, the brushless generator behaves rather differently from the conventional machine.

Any voltages which are induced in the field circuit in the forward direction of the rectifier by a fault occurring in the stator side of the brushless generator will increase the transient current loading of the diodes; voltages in the reverse direction will initially cause a reduction of the forward field current and will be of little consequence until they reach a value sufficient to reduce the total field current to zero. If damage to the diodes is to be avoided, any further increase of reverse voltage must be limited to a value less than the peak transient voltage (p.t.v.) rating of the blocking diodes.

1.3 FAULT CONDITIONS IN BRUSHLESS A.C. GENERATORS

Diode rating is usually specified in terms of maximum continuous forward current, transient current overload capacity and peak inverse voltage. Hence the faults, as regards the diodes, can be classified into two categories:

(a) Faults which cause severe forward current loading of diodes:

1. low resistance fault or a dead short circuit on the d.c. side of the rectifier unit.
2. three-phase short-circuit close to the generator terminals.
3. out-of-phase synchronizing.

(b) Faults which result in large inverse voltage across the diode:

1. "pole-slipping" of a loaded a.c. generator, e.g. due to partial or complete loss of excitation.
2. asynchronous running condition with a periodically varying slip, subsequent to loss of excitation.
3. three-phase short-circuit on the generator terminals.

4. unbalanced short-circuit fault occurring at the terminals of the a.c. generator.
5. "single phasing" of the a.c. generator where it operates on load with one of the stator phases open.

It is well known from the published literature⁶ that the low resistance fault in the field circuit is the worst abnormal current condition in the first category, but fortunately this seldom happens. The next one in the order of severity is the three-phase short circuit.

The most onerous abnormal voltage condition in the second category was found to be^{6,7,8} during the conditions (1) and (2).

One type of faults which occasionally happens in practice, and causes overload of diodes is during "field forcing" by automatic voltage regulator following sudden application of temporary overload on the ^{a.c.} d.c. generator.

1.4 SCOPE OF THE PROJECT

From above abnormal conditions summarized in Section 1.3, the pole-slipping, i.e. when the machine has just lost its excitation, and the asynchronous running condition with a

periodically varying slip, of an initially loaded a.c. generator connected to the busbar through a transformer were selected to be the main subject of this project.

It was tackled both experimentally and theoretically. During tests a laboratory three-phase a.c. generator rated at 69 kVA, 415 V, 1500 rev./min. was used. For the sake of comparison with the behaviour of conventional machines, these abnormal conditions were also observed without rectifier in the field circuit, i.e. with the field winding open. The effects of placing a protective resistance across the field winding, with or without rectifier, were also examined.

Furthermore, the effects of the damping winding on the conditions in the field winding were investigated by removing in stages some of the damper bars first from the quadrature and then from the direct axis.

In all the above conditions, the field current, voltage, armature current and slip were recorded and studied.

On the analytical side, this project is concerned with applying the theory developed by Rao and MacDonald⁷ to predict the behaviour of the a.c. generator with rectifier in the field

circuit when its synchronism is lost due to complete loss of excitation. This prediction involving the use of a comprehensive digital computer programme, was compared with the practically observed behaviour of the machine under test and both were found to be in reasonable agreement. It was found necessary to modify the theory and the computer programme of reference 7 in some respects (mainly with regard to the field current equations) to suit the approach used in this work.

CHAPTER 2

THEORETICAL ANALYSIS OF ASYNCHRONOUS OPERATION WITH RECTIFIER IN FIELD CIRCUIT

2.1 INTRODUCTION

This chapter deals with the theoretical prediction of the behaviour of an a.c. generator with the rectifier in the field circuit, initially on load, following loss of synchronism caused by sudden removal of its excitation. The prediction concerns mainly the voltage and current induced in the field circuit and the variation of speed in this condition, while the machine is connected to the busbar through a transformer.

The method of analysis follows closely that developed by Rao⁷ and MacDonald, but with some modifications which were found necessary, in particular in the field circuit equations.

A set of differential equations is set up, which are similar to the general differential equations of a conventional synchronous machine⁹, but allowing for the rectifier cut off. Because in the condition considered the speed is not constant and is an unknown function of time, the equations become a set of non-linear differential equations which in practice can be solved

only using a digital computer. The following method can be used to predict both the transient condition which follows immediately after the removal of excitation as well as the quasi-steady asynchronous condition eventually reached, in which the machine operates at a periodically varying slip.

The experimental work which checks the validity and accuracy of the theory developed is presented in Chapter 3.

2.2 GENERAL MACHINE EQUATIONS

Fig. 2.1 shows a three-phase synchronous machine with its armature represented as usual by fictitious pseudo-stationary coils on the direct and quadrature axis but with a rectifier in the field winding.

The sign convention and per unit notation adopted for the following analysis is that of Adkins.

Saturation of iron is neglected in this particular case because the machine was operating at only 25% of its rated voltage and at armature current of about rated value.

The extra assumption made in addition to those implied in the two-axis theory is:

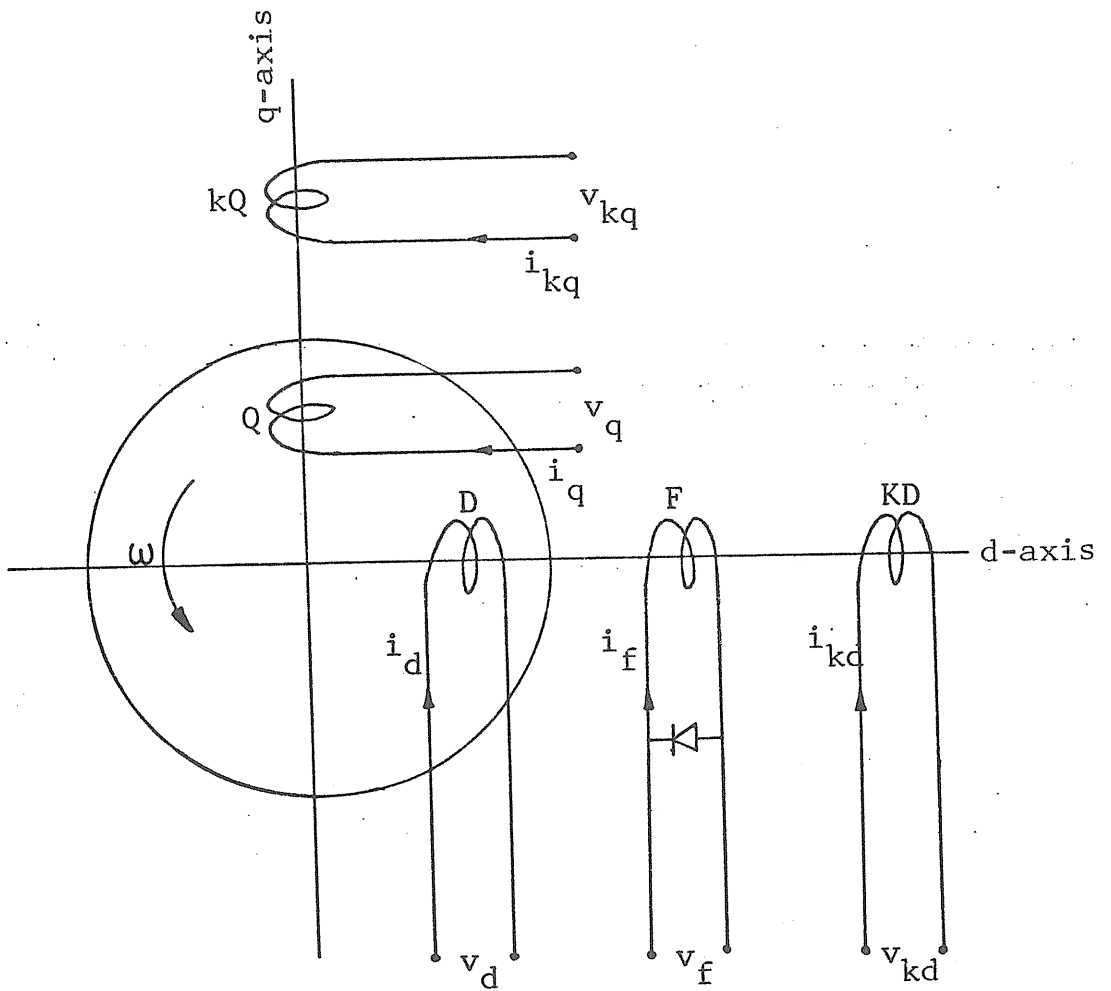


FIG. 2.1

Two axis representation of a three-phase synchronous machine with rectifier in field circuit.

Any external reactance and resistance in the armature circuit (e.g. transformer or transmission line) can be included in the leakage reactance and resistance of the a.c. generator with its terminals assumed to be connected directly to the busbar.

It is important to notice that the changes of speed as well as of $p\psi_d$, $p\psi_q$ terms were fully taken into consideration in the following voltage equations.

The equations describing the generator performance are affected by the presence of the rectifier in so far as the field circuit equations are modified to allow for its presence.

When the rectifier is forward biased the equations are:-

a) circuit voltages:

$$v_f = r_f i_f + p\psi_f \dots\dots\dots(2.1)$$

$$v_{kd} = 0 = r_{kd} i_{kd} + p\psi_{kd} \dots\dots\dots(2.2)$$

$$v_{kq} = 0 = r_{kq} i_{kq} + p\psi_{kq} \dots\dots\dots(2.3)$$

$$v_d = p\psi_d + \omega\psi_q + i_d r_a \dots\dots\dots(2.4)$$

$$v_q = -\omega\psi_d + p\psi_q + i_q r_a \dots\dots\dots(2.5)$$

b) flux linkages:

$$\psi_f = L_f i_f + L_{md} i_{kd} + L_{md} i_d \quad \dots\dots\dots(2.6)$$

$$\psi_{kd} = L_{md} i_f + L_{kd} i_{kd} + L_{md} i_d \quad \dots\dots\dots(2.7)$$

$$\psi_{kq} = L_{kq} i_{kq} + L_{mq} i_q \quad \dots\dots\dots(2.8)$$

$$\psi_d = L_{md} i_f + L_{md} i_{kd} + L_d i_d \quad \dots\dots\dots(2.9)$$

$$\psi_q = L_{mq} i_{kq} + L_q i_q \quad \dots\dots\dots(2.10)$$

When the rectifier is conducting, as in Fig. 2.2(a), the field terminal voltage is equal to the forward drop of the rectifier (v_{dr}):

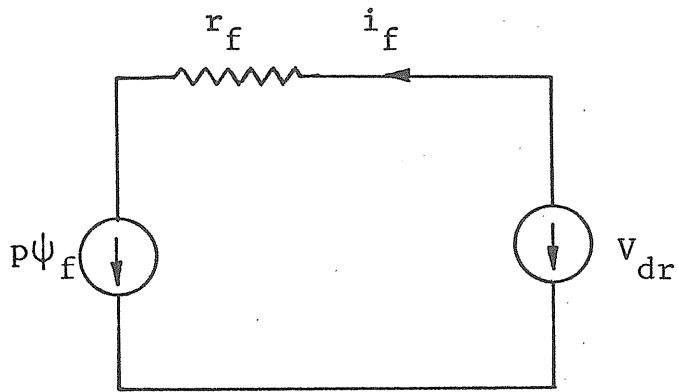
$$v_f = v_{dr} \quad \dots\dots\dots(2.11)$$

In fact, v_{dr} is very small and may be either neglected or for slightly better accuracy taken as:

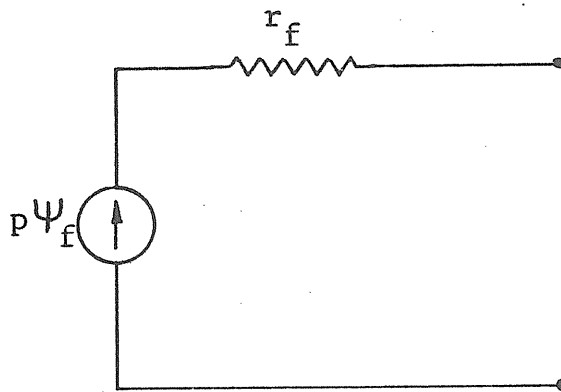
$$v_{dr} = - i_f r_r \quad \dots\dots\dots(2.12)$$

where r_r is the rectifier forward resistance. Because in this particular case the operating point was on the linear part of the rectifier v_{dr}/I characteristic, r_r was assumed constant. Forward field current can be given from equations (2.1) and (2.12):

$$i_f = \frac{v_{dr} - p\psi_f}{v_f} \quad \dots\dots\dots(2.13)$$



(a) Rectifier conducting.



(b) Rectifier blocking: $i_f = 0$.

FIG. 2.2 Effective field circuit of unexcited brushless machine running asynchronously.

The rectifier is forward biased as long as

$$p\psi_f < 0 \quad \dots\dots\dots(2.14)$$

When the rectifier is non-conducting as shown in Fig. 2.2(b), the field current is effectively zero. Hence, substituting $i_f = 0$ in the equations of forward bias, a set of equations for reverse biased condition is obtained as follows:

$$v_f = p\psi_f \quad \dots\dots\dots(2.15)$$

$$v_{kd} = 0 = r_{kd}i_{kd} + p\psi_{kd} \quad \dots\dots\dots(2.16)$$

$$v_{kq} = 0 = r_{kq}i_{kq} + p\psi_{kq} \quad \dots\dots\dots(2.17)$$

$$v_d = p\psi_d + \omega\psi_q + i_d r_a \quad \dots\dots\dots(2.18)$$

$$v_q = -\omega\psi_d + p\psi_q + i_q r_a \quad \dots\dots\dots(2.19)$$

for voltages, and

$$\psi_f = L_{md}i_{kd} + L_{md}i_d \quad \dots\dots\dots(2.20)$$

$$\psi_{kd} = L_{kd}i_{kd} + L_{md}i_d \quad \dots\dots\dots(2.21)$$

$$\psi_{kq} = L_{kq}i_{kq} + L_{mq}i_q \quad \dots\dots\dots(2.22)$$

$$\psi_d = L_{md}i_{kd} + L_d i_d \quad \dots\dots\dots(2.23)$$

$$\psi_q = L_{mq}i_{kq} + L_q i_q \quad \dots\dots\dots(2.24)$$

for flux linkages.

The rectifier is reverse biased if:

$$p\psi_f > 0 \dots\dots\dots(2.25)$$

The electric torque equation for both above conditions is:

$$T_e = \frac{\omega_o}{2} (\psi_d i_q - \psi_q i_d) \dots\dots\dots(2.26)$$

In steady state, $p\psi_f = 0$. Hence $V_{fo} = r_f I_{fo}$, subscript 'o' indicating steady state. In the computer programme the loss of excitation was simulated by application of voltage equal to V_{fo} but of opposite polarity, thus reducing the applied voltage of the field circuit to zero.

2.3 FORMULATION OF PERFORMANCE EQUATIONS FOR ASYNCHRONOUS OPERATION

Because the speed was not assumed constant during pole slipping, the differential equations in Section 2.2 are non-linear but are amenable to step-by-step solution which can be executed by a digital computer. This, however, would require the equations to be rearranged to suit the needs of the computer. The equations are arranged as described in references (10) and (7).

The secondary currents i_{kd} , i_{kq} and i_f and the primary flux linkages ψ_d and ψ_q are to be eliminated from equations (2.1)

to (2.10) for the forward-biased rectifier condition. Eliminating i_f and i_{kd} from equations (2.6), (2.7) and (2.9):

$$\psi_d = (L_d - \frac{L_{md}^2}{L_f})i_d + \frac{L_{md}}{L_f} \psi_f + (L_{md} - \frac{L_{md}^2}{L_f}) \left[\frac{\psi_{kd} - \frac{L_{md}}{L_f} \psi_f - (L_{md} - \frac{L_{md}^2}{L_f})i_d}{(L_{kd} - \frac{L_{md}^2}{L_f})} \right] \dots\dots\dots(2.27)$$

Similarly, by eliminating i_{kq} from equations (2.8) and (2.10):

$$\psi_q = (L_q - \frac{L_{mq}^2}{L_{kq}})i_q + \frac{L_{mq}}{L_{kq}} \psi_{kq} \dots\dots\dots(2.28)$$

Now:

$$\begin{aligned} \omega_o(L_d - \frac{L_{md}^2}{L_f}) &= x'_d \\ \omega_o(L_{md} - \frac{L_{md}^2}{L_f}) &= x'_d - x_a \\ \omega_o(L_{kd} - \frac{L_{md}^2}{L_f}) &= \frac{(x'_d - x_a)}{(x''_d - x_a)} \cdot x_{kd} \\ \omega_o(L_q - \frac{L_{mq}^2}{L_{kq}}) &= x''_q \\ \frac{L_{md}}{L_f} &= \frac{x'_d - x_a}{x_f} \\ \frac{L_{mq}}{L_{kq}} &= \frac{x''_q - x_a}{x_{kq}} \end{aligned}$$

By substituting the above relationship into equations (2.27)

and (2.28) and simplifying:

$$\psi_d = \frac{x_d''}{\omega_o} i_d + (x_d'' - x_a) \left(\frac{\psi_f}{x_f} + \frac{\psi_{kd}}{x_{kd}} \right) \dots\dots\dots(2.29)$$

$$\psi_q = \frac{x_q''}{\omega_o} i_q + (x_q'' - x_a) \frac{\psi_{kq}}{x_{kq}} \dots\dots\dots(2.30)$$

Further, by eliminating i_{kd} , i_{kq} and i_f from equations (2.1), (2.2) and (2.3) a set of equations giving the time-rate of change of the secondary flux linkages is obtained.

$$p\psi_{kd} = \frac{1}{T_{do}''} \left[\frac{x_d' - x_a}{\omega_o} \cdot i_d + \frac{x_d' - x_a}{x_f} \psi_f - \psi_{kd} \right] \dots\dots(2.31)$$

$$p\psi_{kq} = \frac{1}{T_{qo}''} \left[\frac{x_{mq}}{\omega_o} i_q - \psi_{kq} \right] \dots\dots\dots(2.32)$$

$$p\psi_f = v_f + \frac{1}{T_{do}'} \left[\frac{x_d'' - x_a}{x_d' - x_a} \left(\frac{x_{md}}{\omega_o} i_d + \frac{x_{md}}{x_{kd}} \cdot \psi_{kd} \right) - \psi_f \left(1 - \frac{(x_d'' - x_a)}{x_{kd} \cdot x_f} \cdot x_{md} \right) \right] \dots\dots\dots(2.33)$$

The time constants T_{do}'' , T_{qo}'' and T_{do}' are the same as defined by Adkins⁹.

Differentiating equations (2.29) and (2.30) yields an expression for $p\psi_d$ and $p\psi_q$, which then is substituted into equations (2.4) and (2.5) along with the equations (2.29) and (2.30) to obtain a first order differential equation for Pi_d .

Appendix A shows that the primary currents i_d and i_q and the secondary flux linkages ψ_f , ψ_{kd} and ψ_{kq} can be obtained by solving the five simultaneous first order differential equations given in the following equation:

$$\begin{array}{c}
 \left| \begin{array}{l} p i_d \\ p i_q \\ p \psi_f \\ p \psi_{kd} \\ p \psi_{kq} \end{array} \right| = \left| \begin{array}{ccccccccc}
 a_1 & \omega a_2 & a_3 & a_4 & \omega a_5 & a_6 & 0 & a_8 \\
 \omega b_1 & b_2 & \omega b_3 & \omega b_4 & b_5 & 0 & b_7 & 0 \\
 c_1 & 0 & c_3 & c_4 & 0 & 0 & 0 & 1 \\
 d_1 & 0 & d_3 & d_4 & 0 & 0 & 0 & 0 \\
 0 & e_2 & 0 & 0 & e_5 & 0 & 0 & 0
 \end{array} \right| \left| \begin{array}{l} i_d \\ i_q \\ \psi_f \\ \psi_{kd} \\ \psi_{kq} \\ v_d \\ v_q \\ v_f \end{array} \right| \quad (2.34)
 \end{array}$$

Similarly, by eliminating i_{kq} , i_{kd} , ψ_d and ψ_q from equations (2.15) to (2.24) for the reverse bias condition of rectifier, it can be shown that:

$$p \psi_{kd} = \frac{1}{T'_{kdo}} \left[\frac{x_{md}}{\omega_o} i_d - \psi_{kd} \right] \dots \dots \dots (2.35)$$

$$p \psi_{kq} = \frac{1}{T''_{qo}} \left[\frac{x_{mq}}{\omega_o} i_q - \psi_{kq} \right] \dots \dots \dots (2.36)$$

$$p \psi_f = \frac{1}{\omega_o} \left[x_{md} - \frac{x_{md}^2}{x_{md} + x_{kd}} \right] \cdot p i_d + \frac{x_{md}}{x_{md} + x_{kd}} \cdot p \psi_{kd} \dots \dots (2.37)$$

$$\psi_d = \frac{x''_{dr}}{\omega_o} i_d + (x''_{dr} - x_a) \cdot \frac{\psi_{kd}}{x_{kd}} \dots \dots \dots (2.38)$$

$$\psi_q = \frac{x_q''}{\omega_o} i_q + (x_q'' - x_a) \frac{\psi_{kq}}{x_{kq}} \dots\dots\dots(2.39)$$

where T'_{kdo} and x''_{dr} are given by reference 7.

$$T'_{kdo} = \frac{(x_{md} + x_{kd})}{\omega_o \cdot r_{kd}}$$

and

$$x''_{dr} = x_a + \frac{x_{md} \cdot x_{kd}}{x_{md} + x_{kd}}$$

The equations are rearranged; as explained before with equations of forward bias condition, in Appendix B and can be represented as:

$$\begin{vmatrix} p i_d \\ p i_q \\ p \psi_f \\ p \psi_{kd} \\ p \psi_{kq} \end{vmatrix} = \begin{vmatrix} a'_1 & \omega a'_2 & a'_4 & \omega a'_5 & a'_6 & 0 \\ \omega b'_1 & b'_2 & \omega b'_4 & b'_5 & 0 & b'_7 \\ c'_1 & \omega c'_2 & c'_4 & \omega c'_5 & c'_6 & 0 \\ d'_1 & 0 & d'_4 & 0 & 0 & 0 \\ 0 & e'_2 & 0 & e'_5 & 0 & 0 \end{vmatrix} \begin{vmatrix} i_d \\ i_q \\ \psi_{kd} \\ \psi_{kq} \\ v_d \\ v_q \end{vmatrix} \quad (2.40)$$

The matrix (2.34) and (2.40) define the operation of a synchronous machine with a rectifier in its field circuit in terms of the axis quantities.

2.4 STEP-BY-STEP SOLUTION OF MACHINE EQUATIONS

The process of solving non-linear differential equations by

the step-by-step integration method can be summarized

as follows:

1. Selected variables F_i are assumed fixed at a particular instant t_n .
2. Using the values of $F_{i(n)}$ other dependent variables $G_{i(n)}$ are calculated.
3. Using $F_{i(n)}$ and $G_{i(n)}$ the time rate of change of the variables F_i are calculated.
4. The incremental change in the variables F_i over a short period of time Δt are thus obtained and hence the values of $F_{i(n+1)}$ at the following instant $t_{(n+1)}$.
5. Return to step 1 and repeat.

Obviously, the accuracy of a step-by-step integration method of solving differential equations depends to a large extent on the value of the time interval Δt . The smaller the value of Δt , the more accurate the solution, but small Δt means longer execution time and hence the cost of study is increased. In this work, the Kutta-Merson method was used with time interval of 1.0 ms.

2.5 SOLUTION OF MACHINE EQUATIONS USING A DIGITAL COMPUTER

To initiate the programme, some initial values of variables prior to the disturbance (loss of excitation) must be known.

In this case, the steady load condition is defined by the active and reactive powers and the terminal voltage; in addition, the machine parameters are required as data, from which all other quantities referring to the predisturb condition, e.g. voltages, currents and flux linkages, were calculated and used to start the step-by-step process.

The computation is divided into two parts and can be summarised as follows.

a) Condition prior to the disturbance

1. Calculate the armature current and internal load angle ⁹ (δ_g), from which the direct and quadrature axis currents and voltages can be found.
2. Calculate the bus voltage and hence the load angle with respect to busbar voltage.
3. In steady state, $p\psi_f$, $p\psi_{kd}$ and $p\psi_{kq}$ are zero, so from equations (2.31), (2.32) and (2.33) the steady flux linkages are found. Hence, substituting these values into equations (2.29) and (2.30) the steady values of Ψ_d and Ψ_q are obtained.

4. The steady currents (I_d , I_q) and the steady flux linkages (ψ_d , ψ_q) can be used to find the electric torque of the machine using the equation (2.26).

b) Conditions following the disturbance

Loss of excitation is initiated in the computer programme by putting $p\psi_f = -V_{fo}$. During the asynchronous operation the rectifier alternates between conducting and blocking states. The equations for the two modes of operation are formulated in two subroutines called "FORWD" and "REVR". The step-by-step solution of these simultaneous equations is obtained by using the Kutta Merson method, which is incorporated in another subroutine called "INTEG". The transfer of control from one mode of operation to the other is achieved by checking whether $p\psi_f$ is greater or less than zero.

If $p\psi_f$ is less than zero, the "INTEG" subroutine calls for the equations in "FORWD" subroutine to obtain the solution for the forward biased condition.

If $p\psi_f$ is greater than zero, the "INTEG" subroutine calls for the equations in "REVER" subroutine to obtain the solution for the reverse biased state.

2.6 COMMENTS

The method used to analyse the machine's behaviour during asynchronous operation is satisfactory for obtaining conditions immediately following the loss of synchronism, but because of the accumulation of errors in the iterative process used, the prediction of performance during the quasisteady asynchronous running to which the machine settles say 10 s. after the loss of synchronism, may be rather inaccurate and more computer time is required.

Further theoretical studies could be made using this programme to study the effect of various parameters, e.g. damping winding resistance (r_{kd}), the inertia constant (H), external reactance, etc.

The simplified model used could be made more practical, but inevitably also more complicated, by introducing another set of equations which would represent the effect of an a.c. exciter, automatic voltage regulator etc. on the inverse rectifier voltage and forward current, in a study of the machine's asynchronous running due to partial loss of excitation.

CHAPTER 3

EXPERIMENTAL INVESTIGATION OF AN A.C. GENERATOR WITH AND WITHOUT RECTIFIER IN THE FIELD CIRCUIT

3.1 INTRODUCTION

The investigation described in this Chapter deals with the loss of synchronism of a 69 kVA, 415 V a.c. generator, initially on partial steady load, connected to the bus bars through a step-up transformer and subjected to a sudden and complete loss of excitation. This condition was studied with:

- a. The field winding opened.
- b. The field winding closed through a protective resistor.
- c. The rectifier connected across the field winding.
- d. The rectifier and the shunt protective resistor connected together across the field.
- e. The gradual removal of damper bars in stages, first from the quadrature and then from the direct axis, while the rectifier was in the field circuit.

In all the above cases, the induced field voltage, induced field current, slip and line current were recorded, measured and studied.

3.2 PARTICULARS OF A.C. GENERATOR AND ASSOCIATED EQUIPMENT

The laboratory a.c. synchronous generator chosen for this study was a salient pole 3-ph star-connected, 4 poles machine rated at 50 Hz, 1500 rev./min., 69 kVA, 415 V with rotating armature and stationary field member incorporating the damping cage winding. The machine was driven by a directly coupled d.c. compound wound motor (see Appendix C) and was connected to the a.c. busbars through a step-up transformer. A schematic diagram of the test arrangements is shown in Fig. 3.1.

When a brushless a.c. generator excited, e.g. through a 3-phase bridge-connected rectifier and synchronized with the busbars loses its excitation completely, the field circuit can then be regarded as a single rectifying element in parallel with the field winding. Hence only a single diode, connected in parallel across the field winding, was required for these tests instead of the six diodes needed for the normal 3-phase bridge. The silicon diode (BY X 52) used to represent the rectifier bridge was mounted on a heat sink located in the output airstream from the machine, thus ensuring adequate cooling throughout the tests.

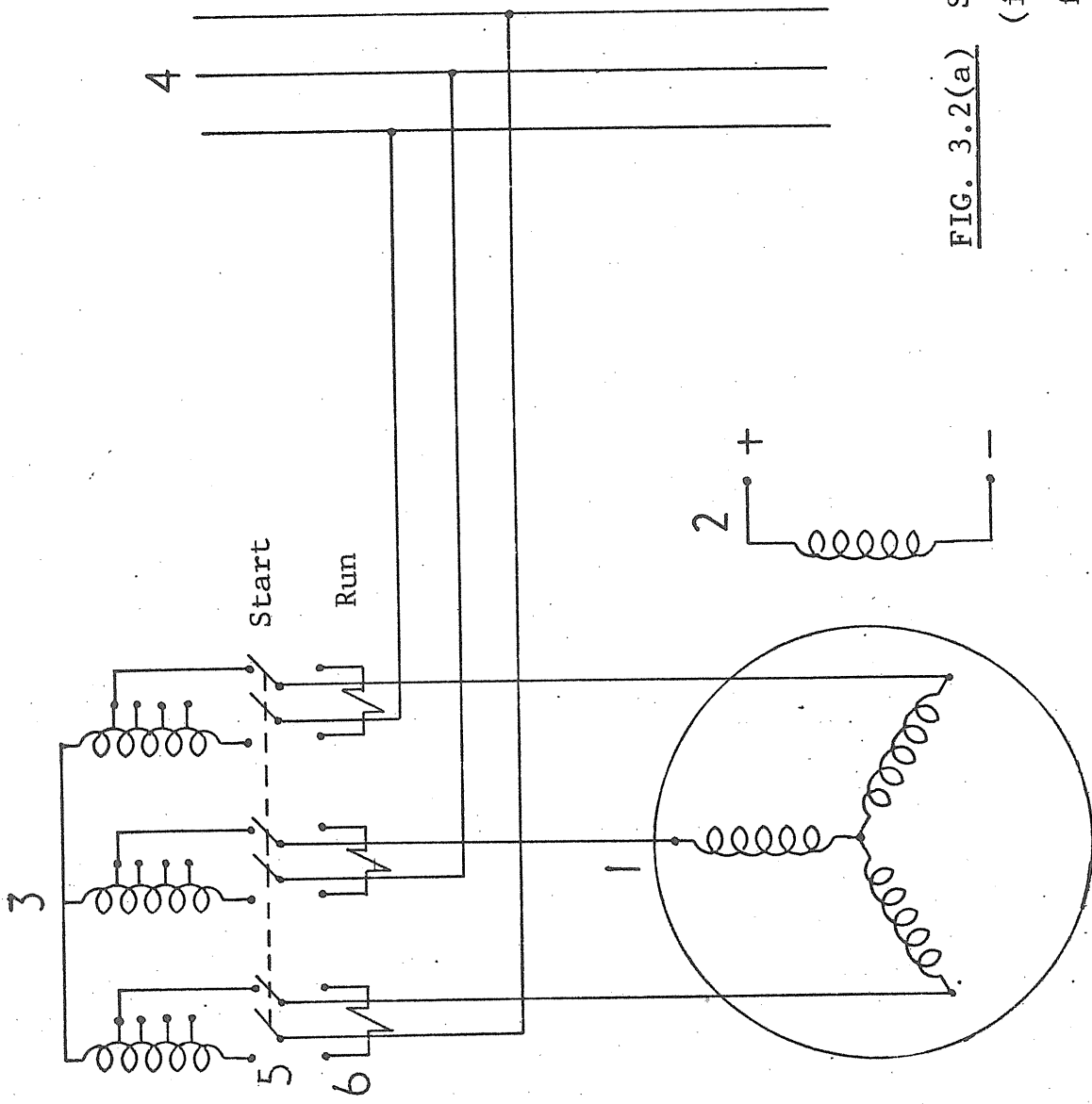
This single silicon diode was connected in reverse bias across the field winding in such direction so as not to short circuit the d.c. supply during steady synchronous operation (see Fig. 3.1).

The loss of excitation was simply effected by disconnecting the d.c. supply from the field winding.

3.3 PRELIMINARY EXPERIMENTAL WORK

The machine set used in this investigation had auxiliary switch gear and control equipment suitable for operation of the synchronous machine in the motoring mode and the d.c. machine as a generator. Thus the synchronous machine was equipped with a three-phase auto-transformer starter incorporating a high-current two-position switch and over-current relays.

Fig. 3.2(a) shows the machine used as a motor. When the switch is in the 'start' position, the machine's terminal voltage would be reduced by the auto-transformer to say 45% of the supply voltage. After the speed builds up, full voltage is applied to the machine by moving the switch to the 'run' position.



1. Synchronous motor armature.
2. Stationary field winding.
3. 3-ph auto transformer.
4. 415 V (line) 3-ph supply.
5. 3-ph two-position two-pole switch.
6. Over-current relay.

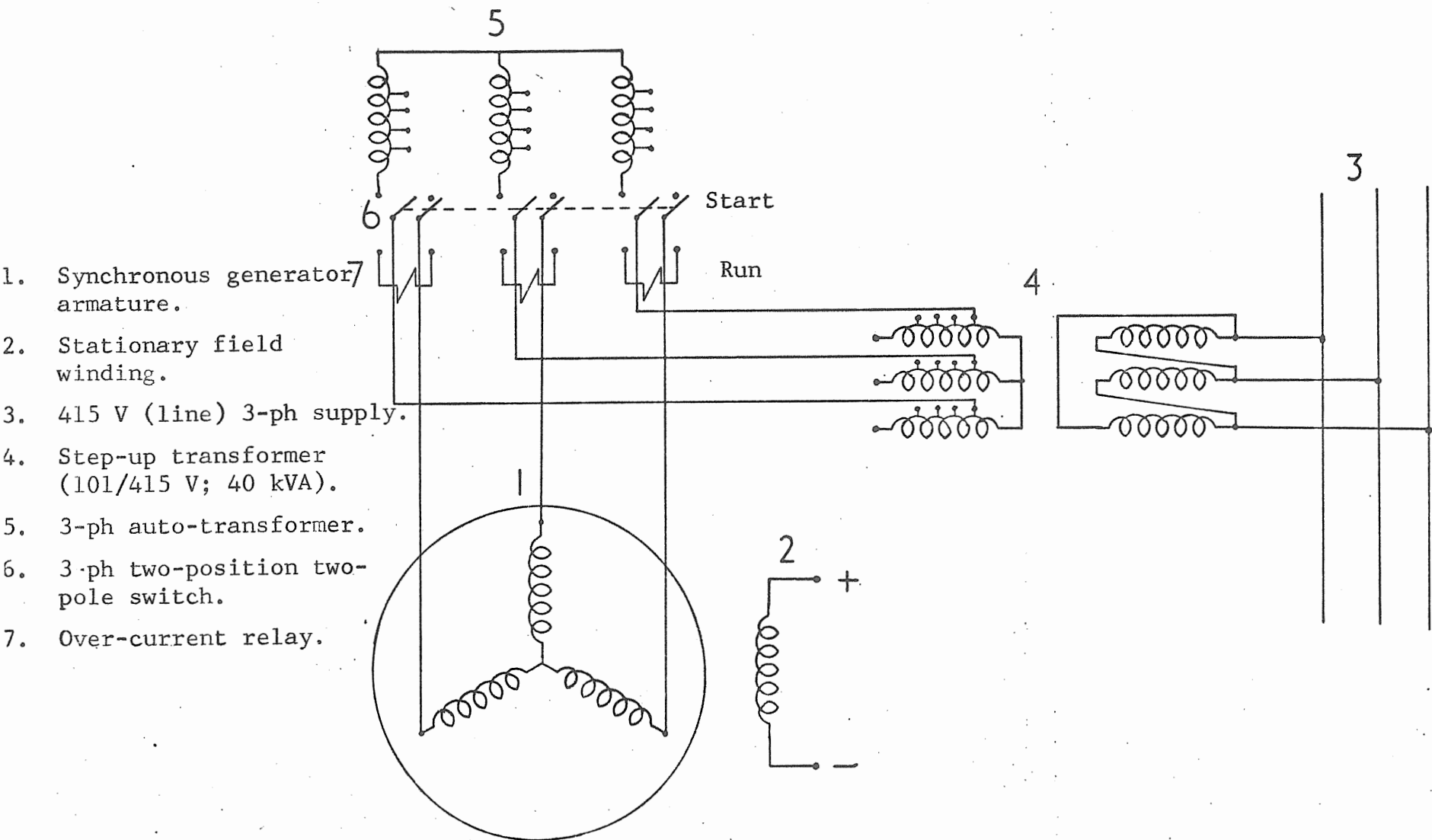
FIG. 3.2(a) Simplified diagram of control switchgear
 (incorporating auto-transformer starter)
 for synchronous machine used as motor.

The first task was to change this circuitry so that the synchronous machine could be operated as a synchronous generator with a separate transformer. Fig. 3.2(b) shows the modified connection where the auto-transformer of the starter was made completely inoperative while still using the starter's high current switch for synchronising purposes.

It is important to notice that because the a.c. generator used is of relatively high rating, the tests could not be carried out at rated voltage or with initial steady load of rated value due to limitations on the magnitude of currents which could be safely drawn from the d.c. and a.c. mains. For this reason, and also in order to reduce the risk of damaging the machines themselves, a 4:1 ratio transformer was inserted between the synchronous machine and the a.c. mains, and also the initial load on it was kept at only about 10% of rated value.

3.4 TEST INSTRUMENTATION AND RECORDING EQUIPMENT

Since during asynchronous operation all currents and voltages fluctuate rapidly and over a wide range of values, a multi-channel ultra-violet recorder was found convenient for simultaneous recording and measurement of all these quantities



- 1. Synchronous generator armature.
- 2. Stationary field winding.
- 3. 415 V (line) 3-ph supply.
- 4. Step-up transformer (101/415 V; 40 kVA).
- 5. 3-ph auto-transformer.
- 6. 3-ph two-position two-pole switch.
- 7. Over-current relay.

FIG. 3.2(b) Modified control switchgear connection for synchronous machine operating as generator.

The induced field voltage was fed to the galvanometer of the u.v. recorder through an attenuator; this had high input impedance and very low output impedance, making it suitable for measuring the voltage across the diode during blocking condition.

A d.c. tachogenerator was used for recording the speed, but the machine available had rather large commutator ripple. Since the speed variations during the asynchronous phenomena under investigation were very small, the corresponding changes in the output voltage of the tachogenerator were also very small and comparable with the magnitude of the commutator ripple.

To overcome this difficulty a filter in the form of a shunt capacitor was connected across the tacho terminals and its output voltage was "backed off" by connecting a d.c. supply in series but with reverse polarity to bring the overall voltage to zero at synchronous speed. Any speed deviation from synchronous value then resulted in a small voltage which was amplified before feeding it into the u.v. recorder.

Figs.3.3 and 3.4 show the actual arrangement of test equipment and associated control gear and instrumentation.

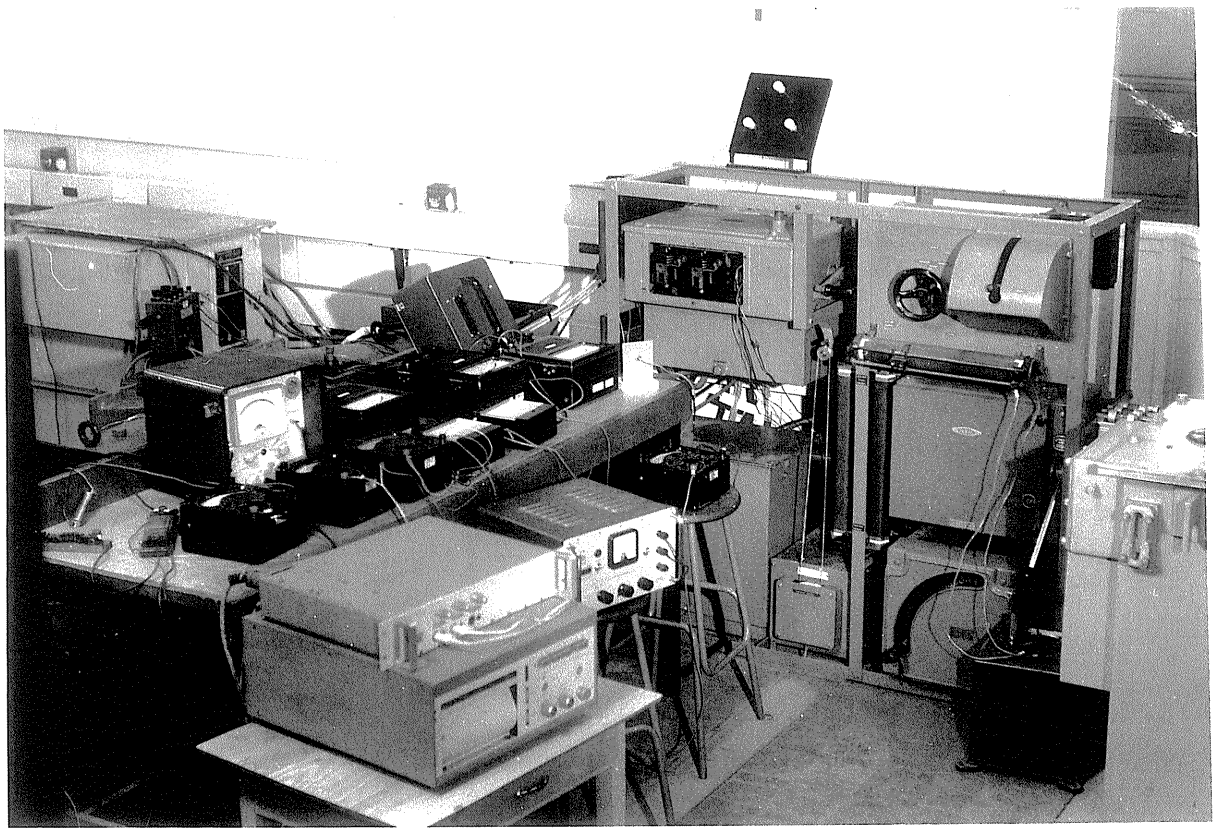


FIG. 3.3 Instrumentation, switchgear and equipment.

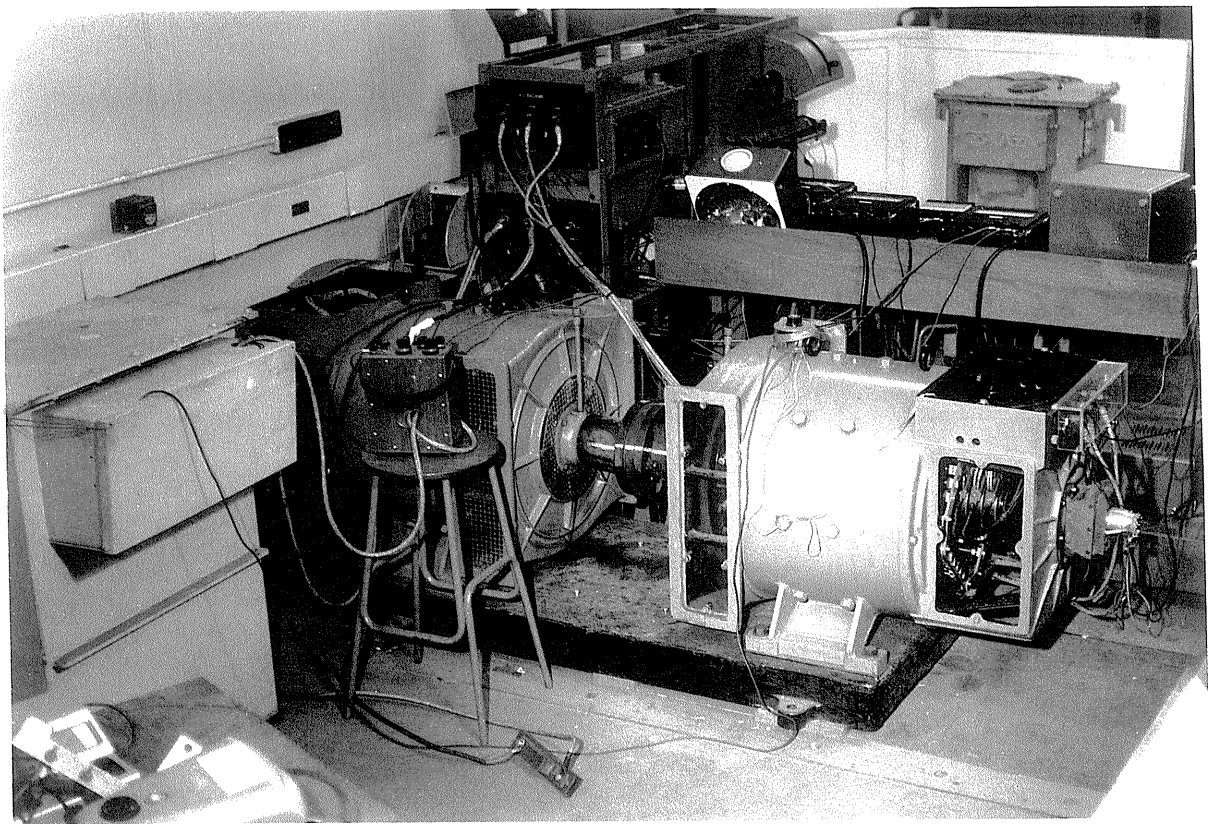


FIG. 3.4 General view of test equipment showing the 69 kVA a.c. generator, the d.c. driving motor and the 40 kVA step-up transformer.

3.5 PROGRAMME OF TESTS AND RESULTS

A series of tests was conducted on a fractionally loaded a.c. generator of 69 kVA rating, connected to the busbars through a step-up transformer with and without rectifier in its field circuit. The main objective of these tests was to study the operation of the generator following its loss of synchronism while it remains connected to the busbars; of particular interest was the transient condition prevailing immediately after the machine falls out of step following the sudden removal of its excitation and its gradual settling down to an asynchronous running condition with a periodically varying slip.

The armature voltage of the driving d.c. motor was maintained constant as well as its shunt field supply which was left unaltered at a preset value corresponding to the initial load on the a.c. generator. All the tests were carried out at the same initial load condition of the a.c. generator: $P = 3.6 \text{ kW}$, $Q = 0.693 \text{ kVAr}$ (lagging) and $V_t = 106 \text{ V}$ (line).

Five major tests were conducted on the a.c. generator, in each of which sufficient time was allowed for quasisteady condition to be established. These tests are presented and studied in the following subsections.

3.5.1 Field Winding Open

The oscillogram in Fig. 3.5(a) shows the time variation of induced field voltage and slip following the loss of excitation supply. The speed rises and eventually settles down to an asynchronous running condition when the machine operates as an induction generator with asymmetrical secondary circuits.

It is important to notice that the speed is not constant but, because of saliency, pulsates about a mean value. An exact analysis of this case requires the solution of a set of non-linear differential equations. The computer programme used for the analysis of asynchronous conditions involving presence of rectifier (see Chapter 2) could be easily adapted to deal also with this case in which the field current remains "symmetrical" during both half-cycles of slip. In practice, at higher values of slip, the fluctuation of speed becomes less significant and to a good degree of approximation, the speed can be assumed constant, hence making the voltage equations linear and therefore can be solved analytically and independently of the torque equation ¹¹.

Due to the difference between the rotor speed and the stator rotating magnetic field, a voltage of slip frequency is

induced in the field circuit. In this case, the half-cycles of field voltage are of equal duration and its value depends mainly on the magnitude of slip.

The trace of induced field voltage (Fig. 3.5(a)) shows exceedingly high harmonics content, and to enable better measurement of the fundamental value of this voltage, a smoothing capacitor (electrolyte $32 \mu\text{F}$, 200 V d.c.) was connected across the field circuit; the voltage trace with harmonics suppressed is shown in Fig. 3.5(b). It can be seen that the peak of induced field voltage is over five times the steady field voltage at the fractional load prior to the loss of excitation; the corresponding mean value of slip eventually reached is 2.6%.

The severe voltage spikes which occur at the instant of loss of excitation and are thought to be due to sudden switching are clearly attenuated by the presence of the smoothing capacitor and possibly also by the response characteristics of u.v. recorder.

The current recorded in one of stator phases for this case of asynchronous operation is shown in Fig. 3.5(c) together with slip.

The synchronous machine (together with its step-up transformer) is assumed to be connected to an infinite bus, which implies that the terminal voltage remained constant and independent of operation of the machine. This assumption is partly confirmed by the fact that throughout the tests the voltmeter readings remained almost constant. The fluctuations of the armature current, which was recorded on u.v. recorder, can be seen to be of relatively low frequency; since the fluctuations of bus voltage would be of the same frequency, which would be 'followed' by the voltmeter, one can conclude that the bus voltage in fact remains constant.

Now, with the field supply removed, the armature current must increase to make up for the reduction of the m.m.f. and raise the net flux linkages with the armature winding to a value needed to induce a voltage approximately equal to the supply voltage. After which the armature current pulsates between maximum and minimum values. It is maximum when the armature m.m.f. acts along the quadrature-axis, and it is minimum when the m.m.f. is directed along the direct-axis.

Moreover, the armature current consists of two components, the magnetizing component to keep the terminals voltage constant, and the other component to balance the effect of eddy currents induced in the iron and damper bars.

3.5.2 Field Winding closed through a protective resistor

The oscillogram of Fig. 3.6 shows the induced field current, slip and the armature current for the same machine running asynchronously, but with field winding closed through protective resistor.

In steady-state synchronous load condition prior to the disturbance, the field and armature flux patterns are stationary with respect to each other, and with constant torque angle between them depending on the power factor. As the excitation is suddenly removed, the field current decays rapidly, thus causing the excitation component of total electromagnetic torque to be appreciably reduced, while the applied shaft torque is still unaltered. Therefore, the machine accelerates and the torque angle starts to increase until it reaches a value where the reluctance torque and the small excitation torque left is insufficient to prevent gradual movement of rotor (for a given setting of d.c. motor). The induced field current due to this movement is by Lenz's Law still positive and thus starts to increase so as to oppose the slipping and tending to resynchronize the machine. But, by now, the torque angle has sufficiently increased for the machine to have entered its unstable region, i.e. the

region where the excitation torque does not follow the torque angle, and hence the resultant net accelerating torque forces the machine to slip its first pole (nearly at $t = 1.5 \text{ S.}$).

After that, the induced field current reverses its direction because the field poles are now facing the armature poles of different polarity. It can be seen that the field current changes its direction every one pole pitch. Eventually, the machine settles down to a pulsating slip operating as an induction generator with its two secondary circuits; one is single phase field winding closed through a resistance and the other is damper cage winding.

It can be seen that the mean slip, which finally the machine settles to, is of smaller value than with the field winding open (see Fig. 3.5(b)) when only the cage winding is effective; this is due to the fact that the net electromagnetic torque with the field winding closed (i.e. when the induced field current can flow) is larger than with the field open, as long as the initial condition of the machine in both cases is the same.

The armature current behaviour can be explained in the same way as with the field winding open, except that the current is larger and has non-sinusoidal envelope. The increase of

current amplitude is explained by analogy to a transformer in which its primary current is larger when the secondary (here field) winding is closed. The reason for non-sinusoidal envelope is the reflection effect of harmonics in the field current.

3.5.3 Field Winding closed through a Rectifier

The oscillogram of the forward field current, inverse voltage and slip is shown in Fig. 3.7(a), with the field winding closed through a rectifier.

Similarly, in order to eliminate the high frequency harmonics in the inverse voltage trace and thus to facilitate measurement of the fundamental value of this induced inverse voltage (which would be predicted by calculation) a capacitor (electrolyte $32 \mu\text{F}$, 200 V d.c.) was connected across the field circuit. The effect of the capacitor is shown in Fig. 3.7(b).

The presence of the rectifier causes the two cases studied in Subsection 3.5.1 and 3.5.2 to occur alternately; the same approach used to explain the observations of the previous two tests can still be applied in some respects to the present case.

As the field supply is switched off, the field current again decays exponentially, but this time with a much longer time constant because now the field circuit is effectively short-circuited.

The excitation torque component reduces according to the change in the field current. Again, the reluctance torque together with the small excitation torque left is insufficient to stop the gradual movement of the rotor (for given setting of d.c. motor), hence the torque angle starts increasing steadily.

Due to this relatively small movement as well as transformer voltage, the induced field current starts building up by

Lenz's Law in a positive direction so as to produce an excitation torque which will oppose the change in the speed. But the torque angle has by now sufficiently increased, and thus the machine is in the unstable region, where the excitation torque does not follow the torque angle, and hence the net accelerating torque forces the machine to slip its first pole (nearly at $t = 4$ S).

After this, the field poles are facing armature poles of different polarity, and so the field current tends to

reverse its direction but is obviously prevented from doing so by the blocking action of the rectifier, and therefore it is forced to zero. Slipping of successive poles can be clearly seen in the record of armature current, Fig. 3.7(c). During the period of zero field current, the relative speed is comparatively large, and hence induces a large inverse voltage across the rectifier. The peak inverse voltage is over 3.5 times that of fractional load prior to loss of excitation.

As the slip continues to increase, the field poles move towards the next poles of polarity different from the previous one, hence the field current is able to flow again. This positive forward induced field current tries to destroy its cause by Lenz's Law and attempts to resynchronize the machine, i.e. to reduce the slip. Due to this violent reduction in the slip, the machine's slip drifts into the negative region.

Negative slip means that the machine is operating at sub-synchronous speed and hence the field poles are passing the "same" corresponding armature poles but in reverse direction, thus the induced field current tries to reverse its direction, but the blocking of rectifier reduced it to zero.

With the field current reduced to zero, the corresponding excitation torque is also zero, hence the machine starts to accelerate again, and due to this relative movement the field current starts building up again and similar slip cycle is repeated. It can be seen that the two slip cycles shown are not of equal duration. The first slip cycle represents the transient period for the machine, i.e. the slip cycle which immediately follows the loss of excitation, after which the machine settles down to a quasisteady asynchronous condition with periodically varying slip.

The record of armature current is shown in Fig. 3.7(c). The behaviour of armature current can be explained in the same manner as before. As the excitation is removed (after the initial transient is over), the a.c. supply provides more armature current to maintain the terminal voltage constant. Thereafter, the armature current response to the field current variations.

The armature current, as before, consists of two components; the magnetizing component to look after the terminal voltage, and the other component changes with the currents induced in the field circuit. With the rectifier conducting, the armature current has to balance the effect of forward field current and eddy currents induced in the iron and damper

bars, while during the blocking period the armature current only balances the eddy currents. That is why the armature current is more with rectifier conducting than with it blocking.

3.5.4 Rectifier shunted by a Protective Resistor across the Field Winding

Fig. 3.8(a) shows an oscillogram of the forward field current, inverse voltage and slip for an a.c. generator running asynchronously, whose field is closed through a rectifier shunted by a protective resistor.

Initially, with the rectifier conducting, the behaviour of the forward field current, slip and armature current (shown in Fig. 3.8(b)) are the same as those presented in Subsection 3.5.3 because the protective resistor is short-circuited by the conducting of rectifier, whereas with the rectifier blocking, the curves behave rather differently.

When the rectifier is non-conducting, the protective resistor provides a path for the negative field current to flow, hence the inverse voltage is considerably reduced. Usually, the value of protective resistor is taken as 5-10 times the field resistance. Because the brushless machine has its diodes

mounted on the shaft, the protective resistor (if required) has to be permanently connected across the field circuit; this means of course that the resistance must have a compromise value (as mentioned above) on the one hand not to draw excessive current from the excitation supply during steady-state operation of the machine, and on the other hand not to become less effective in protecting the rectifier by having too high value.

3.5.5 Effects of modifying damping winding

For the purposes of another research project, the damping cage winding of the particular machine used was modified in such a manner as to enable any bar to be individually isolated.

With the machine running asynchronously due to complete loss of excitation and with quadrature-axis damping circuits disconnected, the peak inverse voltage, forward field current and slip were recorded.

As was expected, the induced field current and inverse voltage were only slightly increased by removal of the quadrature-axis damping because they have little screening effect on the field

winding. Moreover, the cage torque produced by the interaction of the currents induced in damper bars and the armature current, was obviously slightly reduced, and hence the machine slipped its first pole in less time compared with that of Fig. 3.7(b). The traces for this condition are NOT shown because of their similarity to those in Fig. 3.7(b).

As far as the direct-axis bars are concerned, they constitute a magnetic screen for the field windings and thus contribute a significant portion of the armature balancing m.m.f. So any change in the direct axis bars will then affect the slip, induced field current and the inverse voltage. Fig. 3.9(a) shows the effects of disconnecting 2/5 of the direct-axis bars from each pole, while the quadrature-axis bars are reconnected. The inverse voltage is increased by 10%.

Furthermore, the effects of removing all the damping bars were also observed and this is shown in Fig. 3.9(b). Now, only one secondary circuit (i.e. field winding) is left, which faces directly the armature current m.m.f. and hence the induced voltage and current are appreciably increased. The peak inverse voltage is increased by about 25%. Also it can be seen that the period of slip cycle is considerably reduced because the cage torque is now zero (the effect of

any eddy currents in iron are still present); hence the net accelerating torque increases, which obviously forces the machine to slip more rapidly.

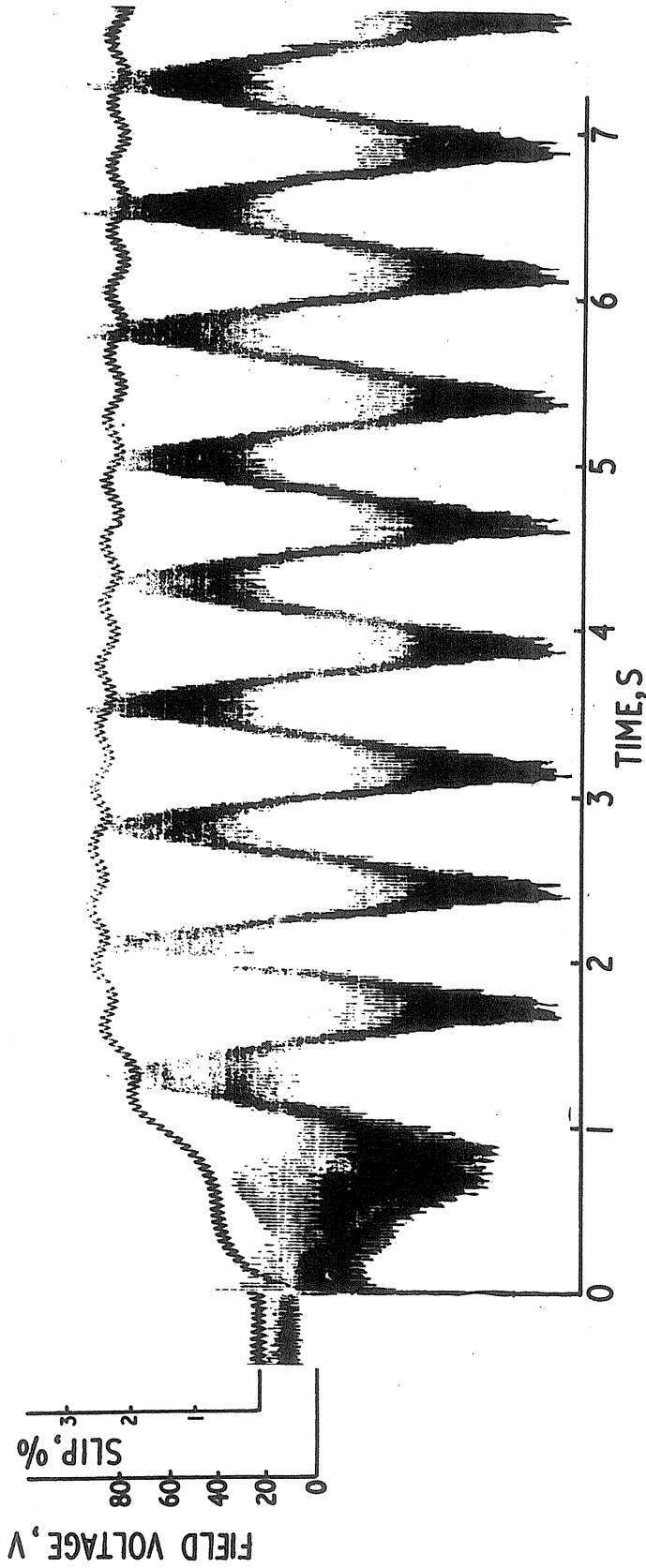


FIG. 3-5(d) ASYNCHRONOUS OPERATION OF A 69KVA 415V A.C. GENERATOR.

FIELD WINDING OPEN

LOAD CONDITION PRIOR TO LOSS OF EXCITATION

$$P = 3.6 \text{ kW} ; Q = 0.693 \text{ kVAR (lag)}$$

$$V_t = 106 \text{ V} ; N = 1500 \text{ rev/min.}$$

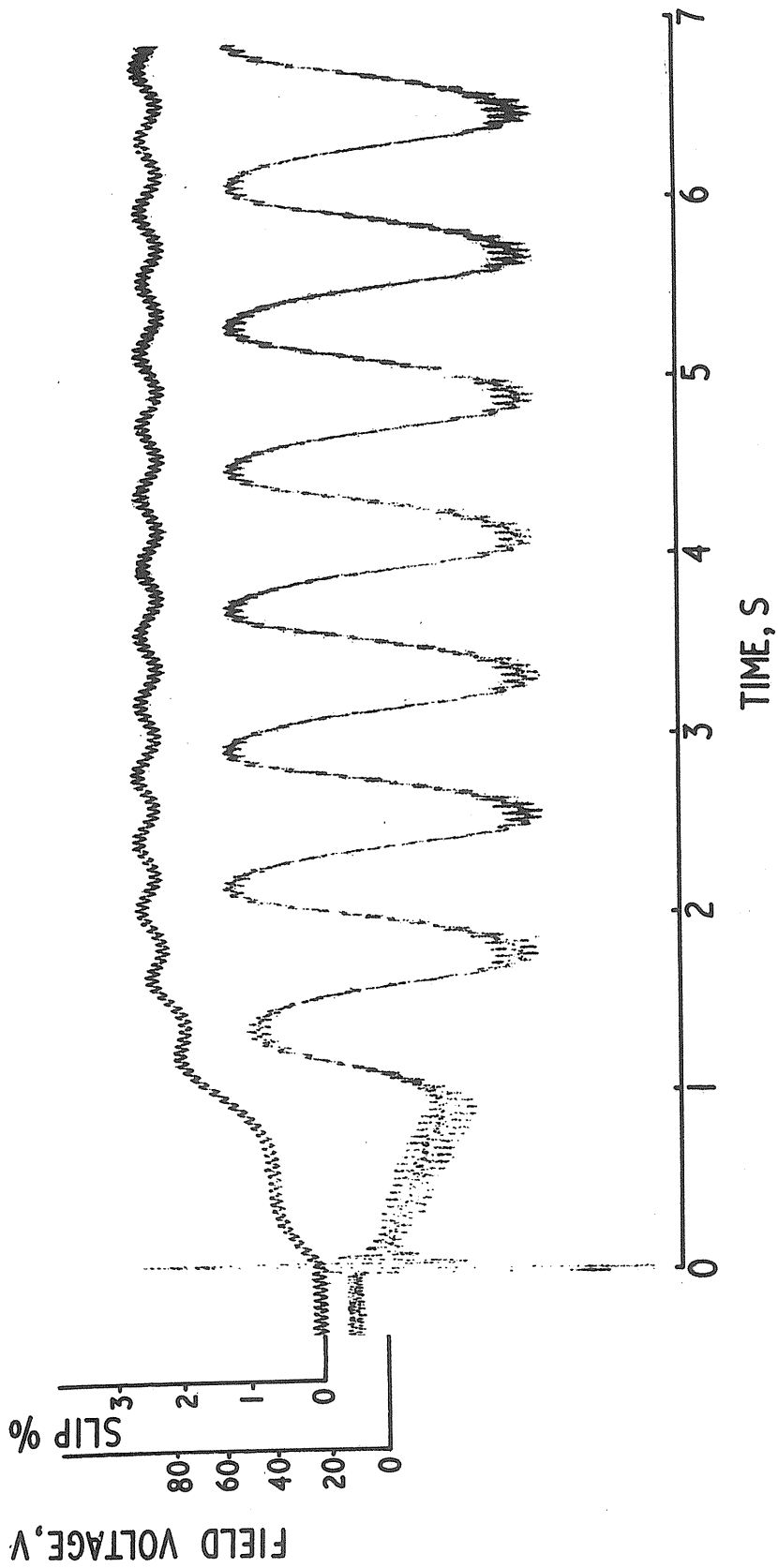


FIG. 3.5(b) WITH SMOOTHING CAPACITOR ACROSS FIELD WINDING

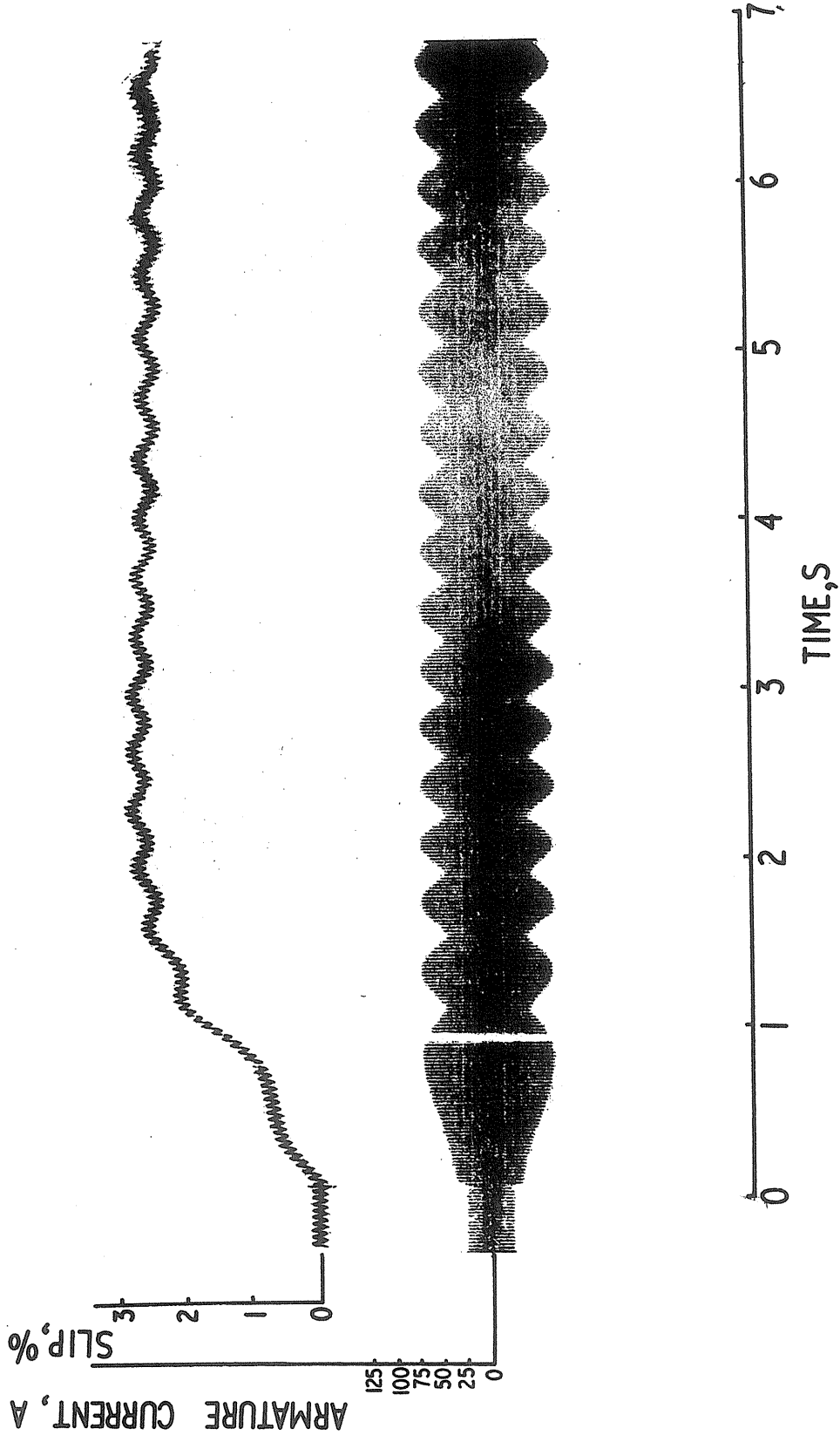


FIG. 3.5(c) RECORD OF ARMATURE LINE CURRENT

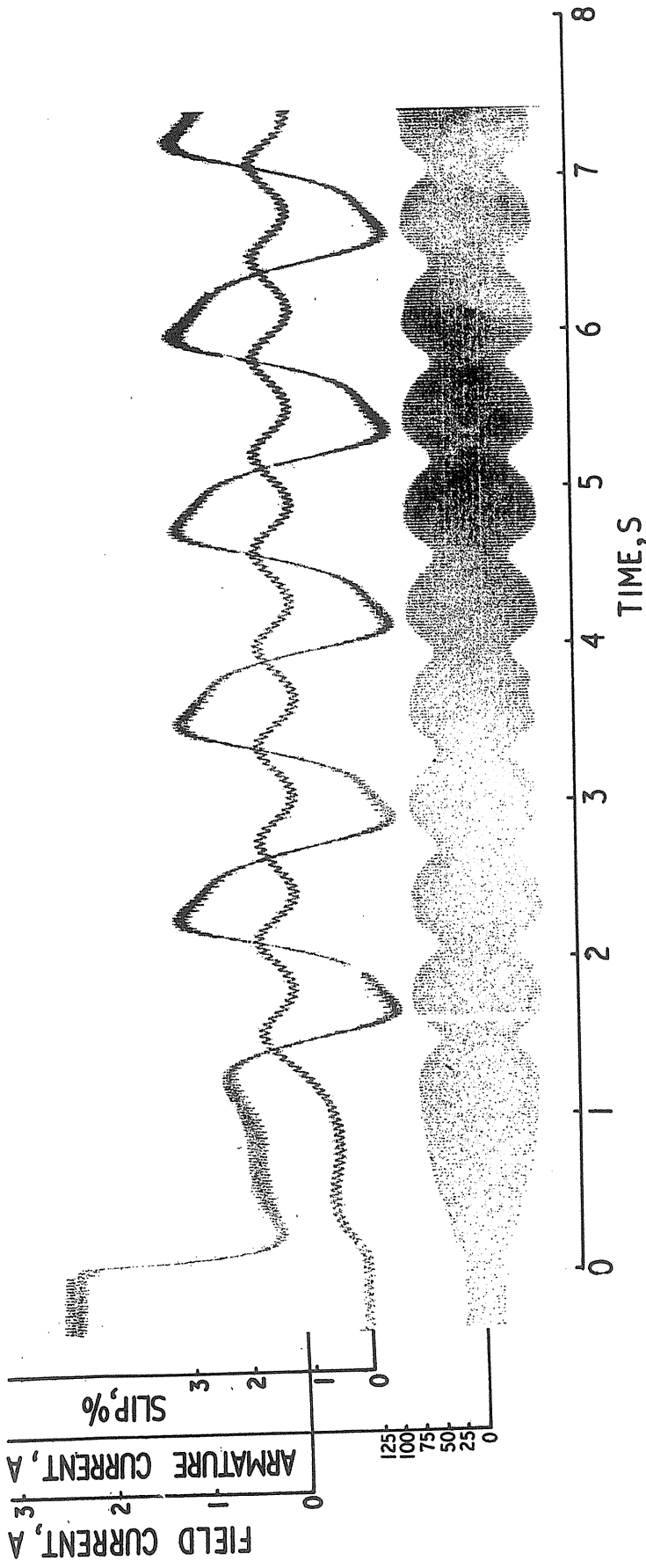


FIG. 3-6 ASYNCHRONOUS OPERATION OF A 69 kVA, 415 V A.C. GENERATOR WITH ZERO EXCITATION.
FIELD WINDING CLOSED THROUGH PROTECTIVE RESISTOR $R_p = 4 \times R_f$

LOAD CONDITION PRIOR TO LOSS OF EXCITATION

- P = 3.6 kW ; Q = 0.693 kVAR (lag.)
- $V_t = 106$ V ; N = 1500 rev/min.

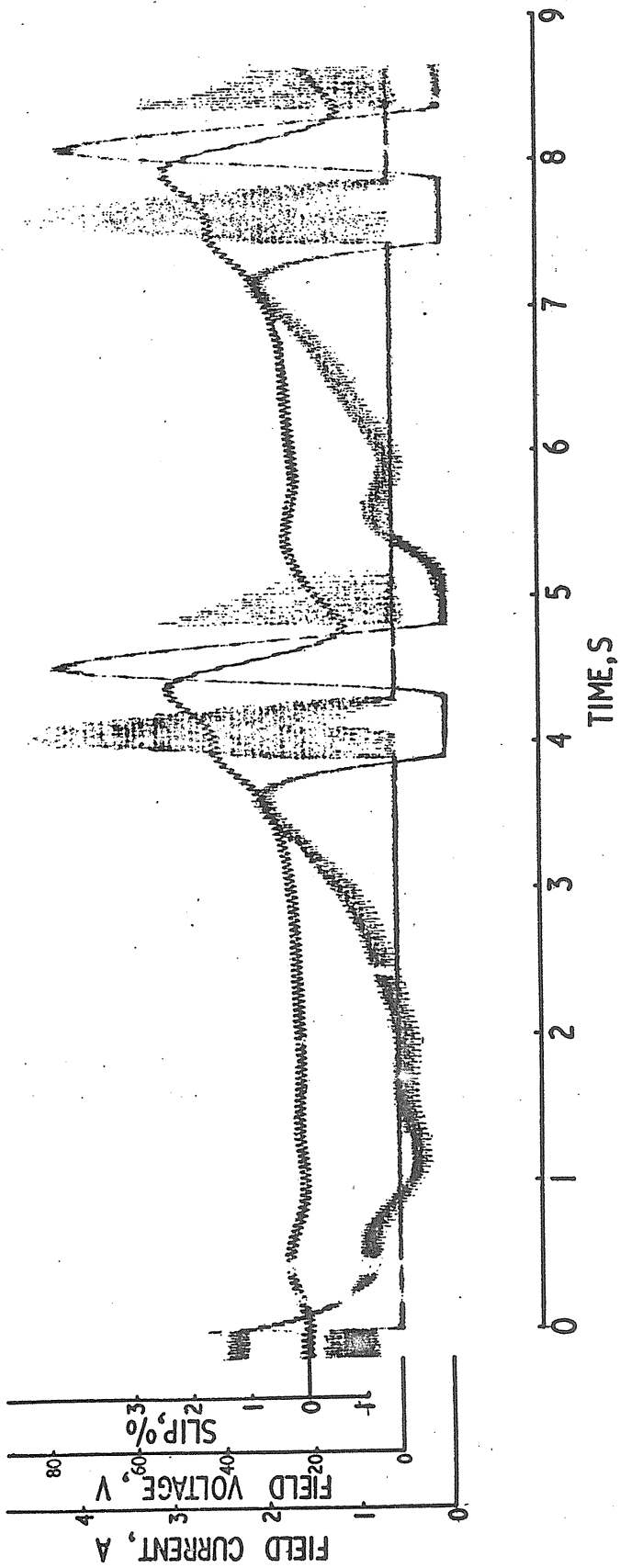


FIG. 3.7 (a) ASYNCHRONOUS OPERATION OF A 69 kVA, 415 V A.C. GENERATOR WITH ZERO EXCITATION.

FIELD WINDING CLOSED THROUGH RECTIFIER

LOAD CONDITION PRIOR TO LOSS OF EXCITATION

$P = 3.6 \text{ kW}$; $Q = 0.693 \text{ kVAR (lag)}$
 $V_t = 106 \text{ V}$; $N = 1500 \text{ rev/min.}$

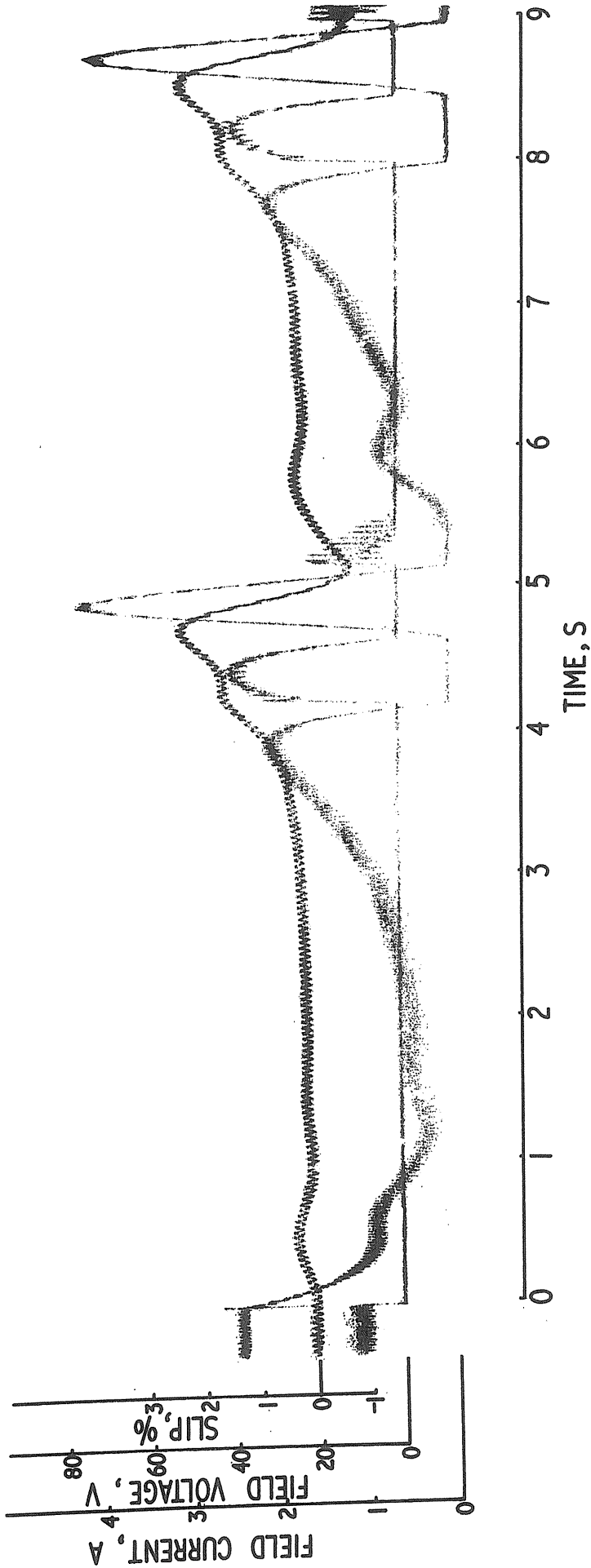


FIG. 37 (b) WITH SMOOTHING CAPACITOR ACROSS FIELD WINDING

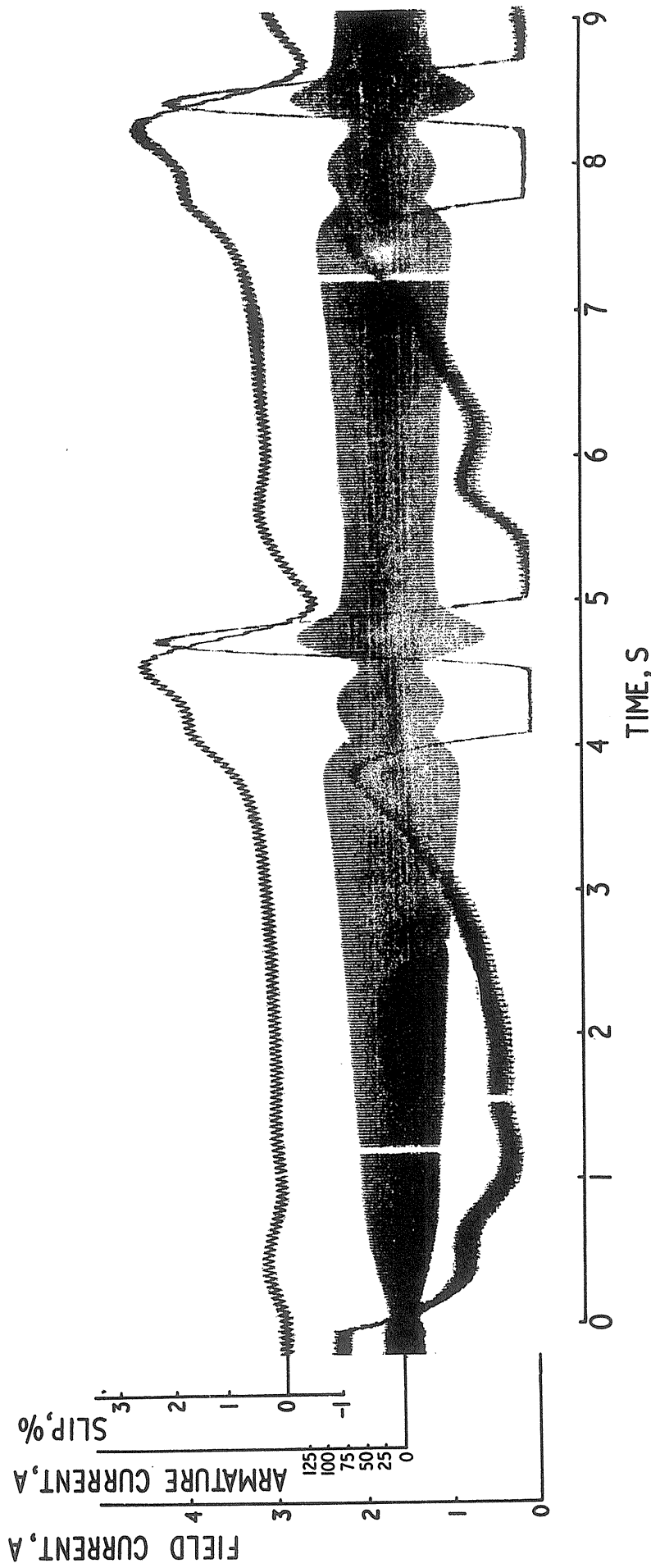


FIG. 3-7 (c) RECORD OF ARMATURE LINE CURRENT

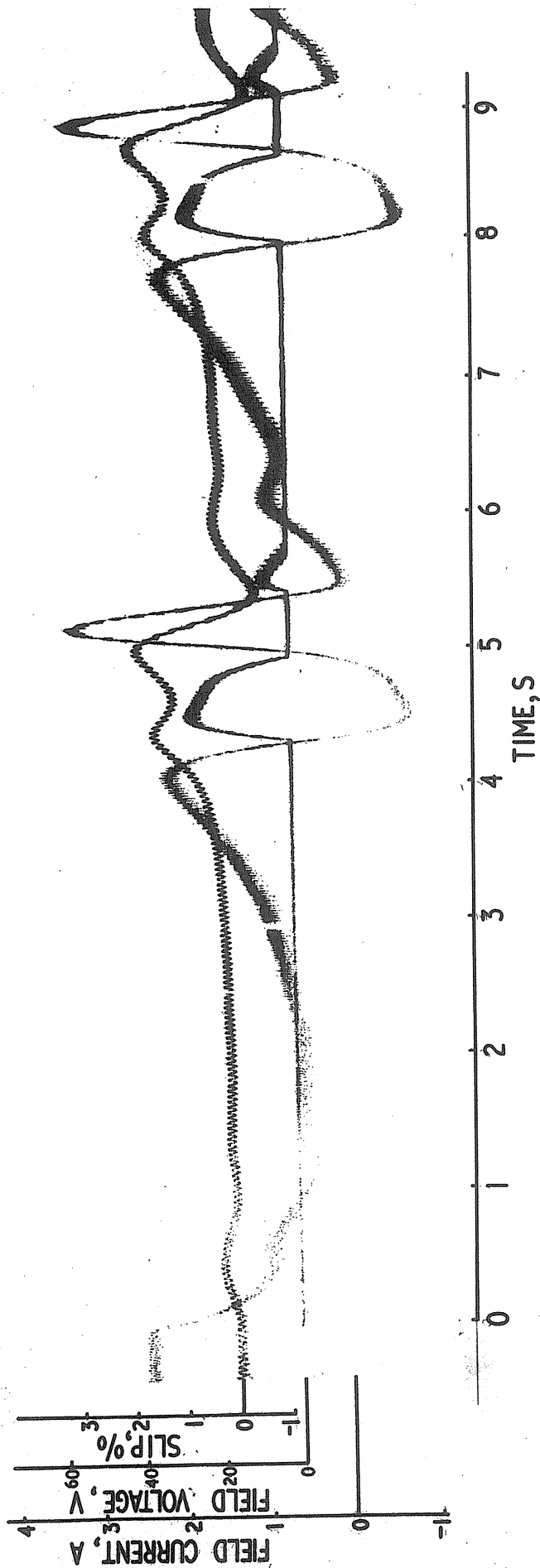


FIG. 3-8(a) ASYNCHRONOUS OPERATION OF A 69 kVA, 415 V AC GENERATOR WITH ZERO EXCITATION.

FIELD WINDING CLOSED THROUGH RECTIFIER SHUNTED BY PROTECTIVE RESISTOR $R_p = 4 \times R_f$

LOAD CONDITION PRIOR TO LOSS OF EXCITATION

$P = 3.6 \text{ kW}$; $Q = 0.693 \text{ kVAR(lag)}$

$V_t = 106 \text{ V}$; $N = 1500 \text{ rev/min.}$

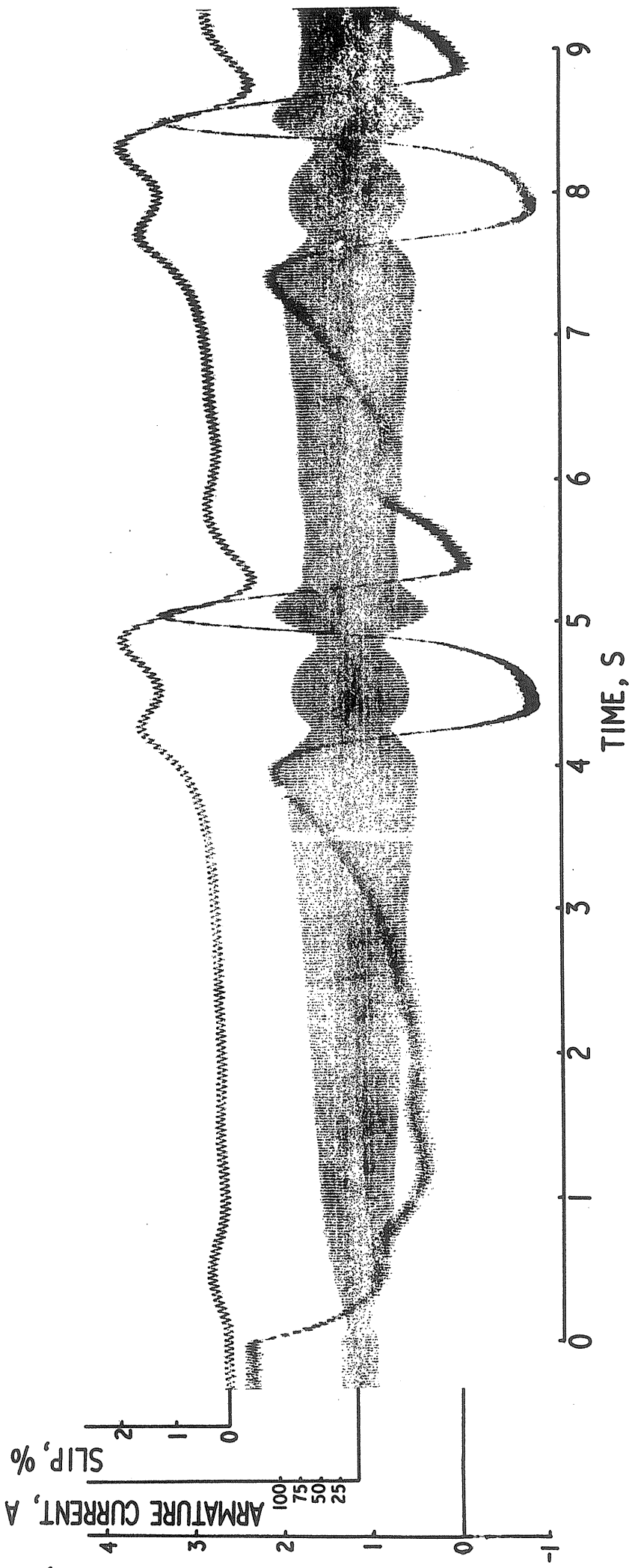


FIG. 3-8 (b) RECORD OF ARMATURE LINE CURRENT

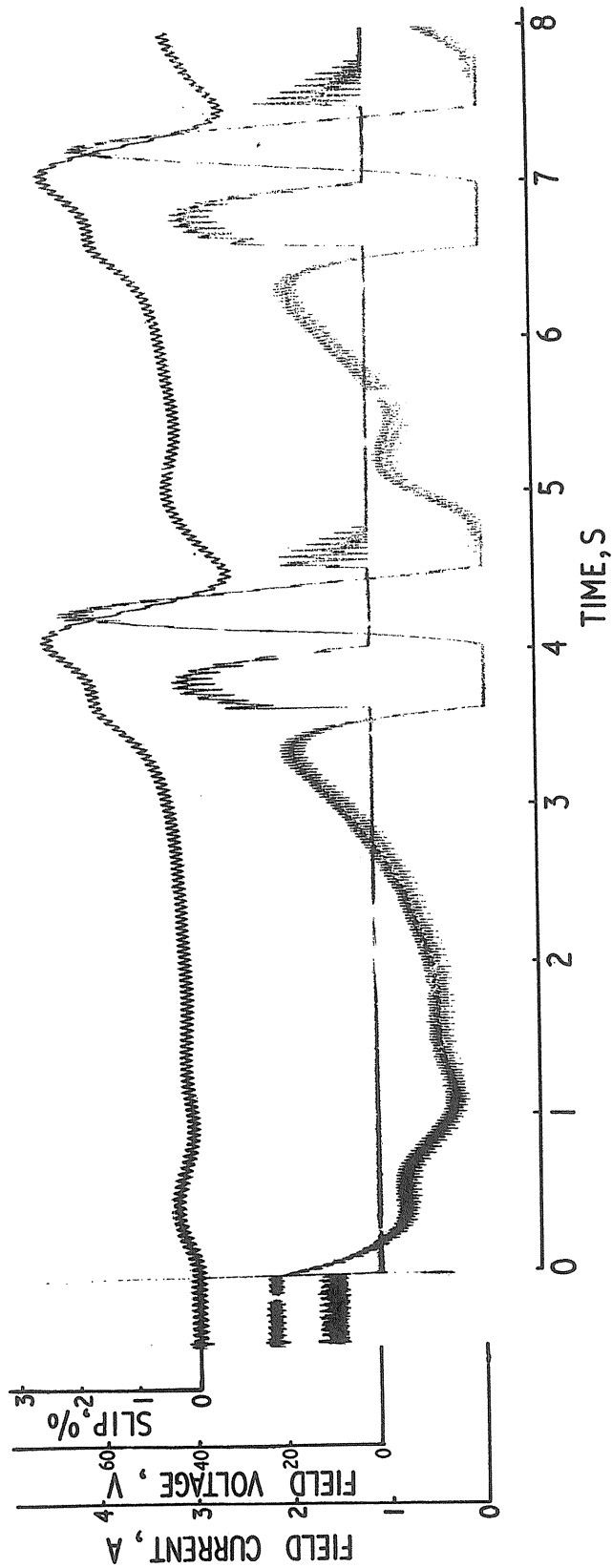


FIG. 3-9 (a) ASYNCHRONOUS OPERATION OF A 69 kVA, 415V A.C. GENERATOR WITH ZERO EXCITATION.

FIELD WINDING CLOSED THROUGH RECTIFIER

2/5 DAMPING WINDING BARS ON DIRECT-AXIS DISCONNECTED

LOAD CONDITION PRIOR TO LOSS OF EXCITATION

$P = 3.6 \text{ kW}$; $Q = 0.693 \text{ kVAR (lag.)}$

$V_t = 106 \text{ V}$; $N = 1500 \text{ rev/min.}$

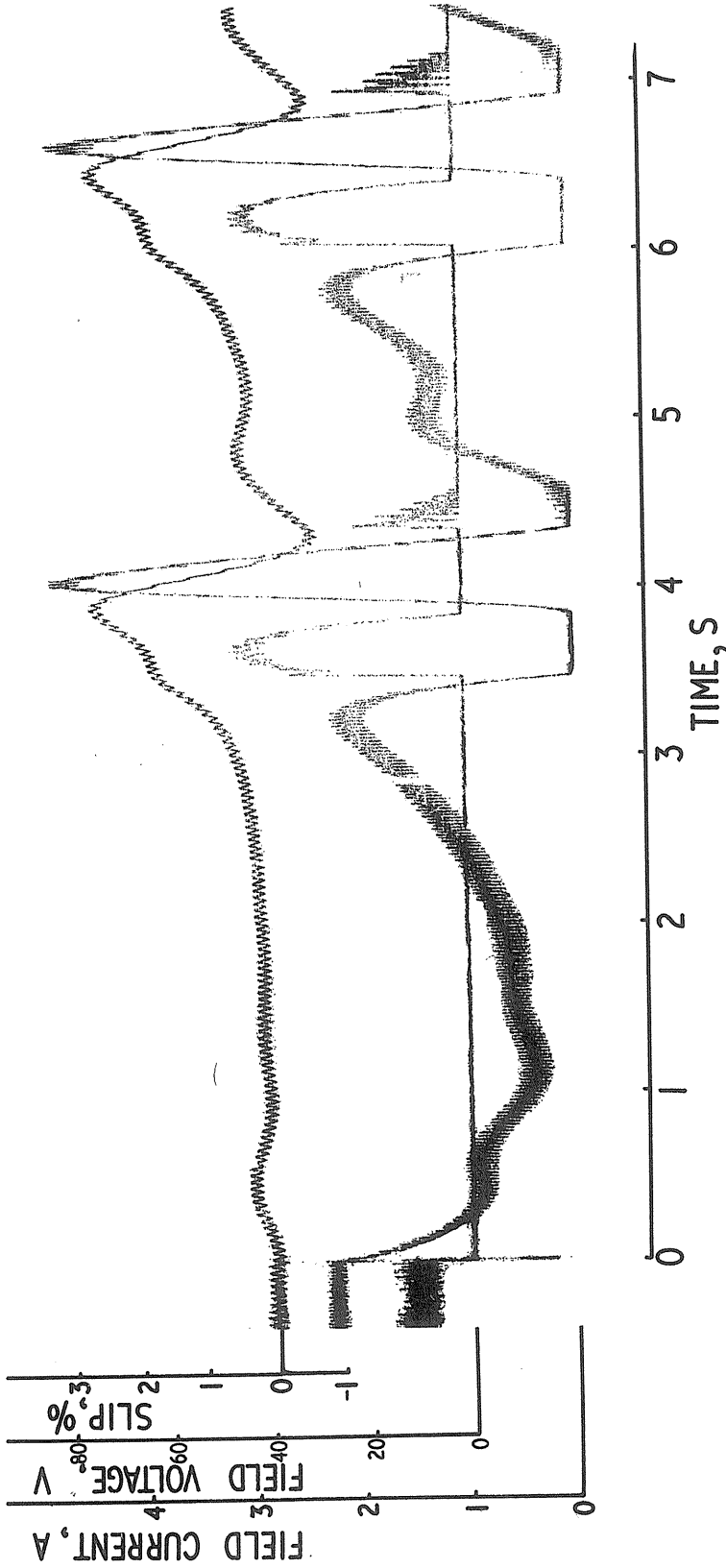


FIG. 3-9 (b) FIELD WINDING CLOSED THROUGH RECTIFIER
DAMPING BARS DISCONNECTED

CHAPTER 4

DISCUSSIONS AND CONCLUSIONS

4.1 COMPARISON BETWEEN TESTED AND COMPUTED PERFORMANCE

In Figs. 4.1(a) and 4.1(b) the theoretical and experimental values of forward field current, inverse voltage and slip are plotted for comparison.

The following observations can be made after studying the differences between the tested and computed results:

- 1) A discrepancy of less than 10% between the maximum amplitudes of the field current.
- 2) A difference of about 15% in the values of the peak inverse voltage.
- 3) Although the computed duration of the first slip cycle (i.e. slip cycle which represents the initial transient asynchronous operation of the machine) does agree reasonably with the test one, but during the subsequent quasisteady asynchronous operation of the machine, the discrepancy is noticeably larger.

Nevertheless, the overall agreement between the theoretical and experimental characteristics is such as to indicate that

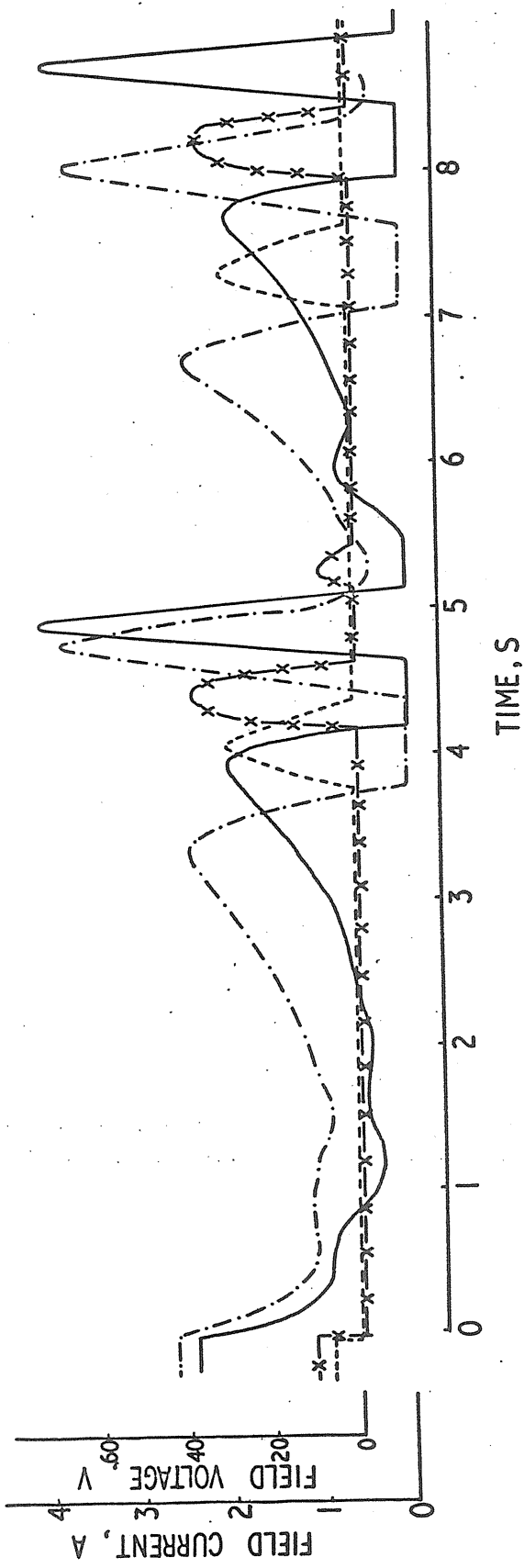


FIG. 4-1(a) COMPARISON OF TESTED AND PREDICTED RESULTS FOR ASYNCHRONOUS OPERATION OF A 69 kVA 415V A.C. GENERATOR WITH ZERO EXCITATION.

FIELD WINDING CLOSED THROUGH RECTIFIER

FIELD CURRENT	INVERSE VOLTAGE
— TEST	--- TEST
- - - - CALCULATED	- - - - CALCULATED

LOAD CONDITION PRIOR TO LOSS OF EXCITATION

P = 3.6 kW : Q = 0.693 kVAR (lag)

b = 0.001 : c = 0.001 (AVAR)

EXCITATION

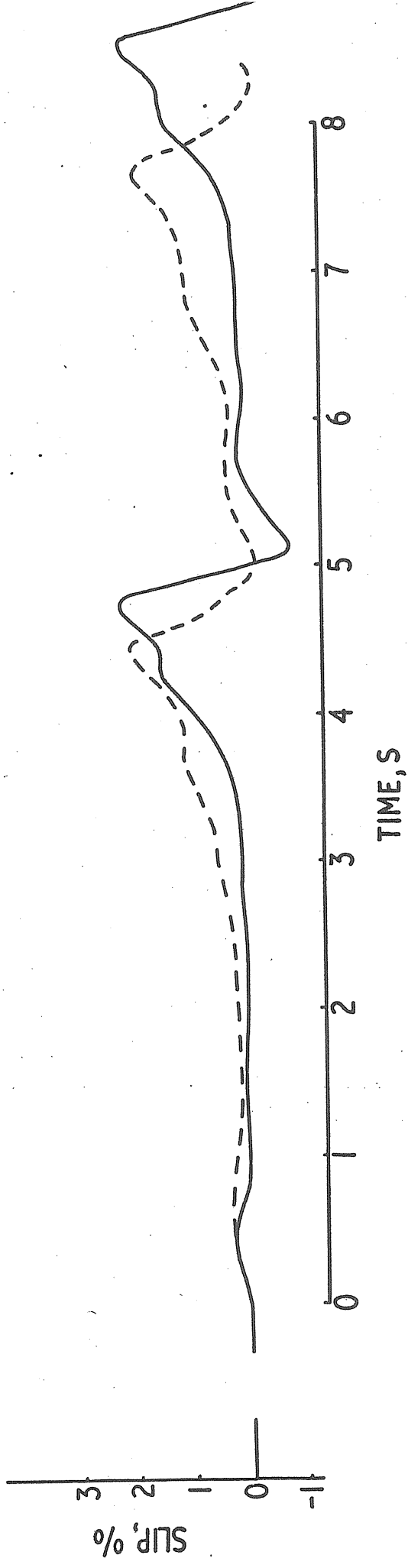


FIG. 4-1 (b) RECORD OF SLIP

----- TEST ——— CALCULATED

the adopted method of analysing asynchronous operation of an a.c. generator with rectifier in the field circuit is basically sound.

The main reasons for the deviation between the tested and predicted results are thought to be:

- 1) The fact that, as data for the theoretical computer prediction, the basic design parameters of the synchronous generator and the associated transformer (listed in Tables 1 and 2 respectively) were used, without having been verified by testing.
- 2) Other derived parameters such as x_d' , x_d'' , x_q'' , T_d' , T_d'' , etc. which appear in the performance equations, were calculated by a separate subroutine using formulae given in Ref. 9, which themselves involve approximations. Again, these parameters could (if time permitted) be obtained by test, e.g. sudden 3-ph short-circuit, static impedance test, etc.
- 3) The design parameters, as specified by manufacturers, and as used in the computation, referred to the original cage winding. This winding was in fact modified as mentioned earlier (see Subsection 3.5.5) for the purposes of another research project.

- 4) The field and damper winding design parameters were given in per unit values, without any clear indication as to what base values were used. The computer programme requires the parameters in SI units and it is likely that the base values used for the conversion of these parameters did not agree with that applied by the manufacturer.
- 5) The losses of the a.c. generator were obtained by assuming the value of the efficiency. For better results these losses should be determined by the usual tests.
- 6) The speed-torque characteristic of the prime-mover (d.c. motor) was again assumed, but it could be determined more accurately by test. Because of very small range of slip, the error introduced by this assumption is bound to be small. On the other hand, the d.c. motor was in fact in dynamic state and there is doubt as to what extent the steady speed-torque characteristic applied.

On the experimental side, it was rather difficult to record precisely the steady-state load condition prior to loss of excitation. This was because the machine was operated at only 25% of rated voltage, in which condition the wattmeter readings were oscillating noticeably.

Also, it was possible that the magnitude of the inverse voltage was slightly affected by the use of a capacitor

connected across the rectifier to obtain the fundamental value of inverse voltage (see Subsection 3.5.3). However, the possibility of this error was eliminated by checking that the filtered wave form of inverse voltage remained substantially unaltered when much bigger values of capacitance were tried.

4.2 CONCLUSIONS

In this project, the behaviour of a partially loaded a.c. generator running asynchronously, due to sudden removal of its excitation, while it remains connected to the busbars, was studied. The time variation of induced field voltage and current, slip and armature line current in this condition have been recorded, measured and a considerable effort was made to obtain a convincing explanation in physical terms for the observed behaviour.

This experimental study of the asynchronous operation covered both the configuration of the field current applicable to the conventional machines as well as that of machines with brushless excitation scheme, i.e. with rectifier in the field circuit. The main conclusions arrived at on the basis of these studies are as follows:

- 1) It takes a longer time for the machine to lose synchronism (or rather "slip its first pole"), if a closed conducting path for the field current is maintained after removal of the excitation supply.

This was confirmed by the fact that the machine lost its synchronism most rapidly when its field winding was left open. When a conducting path for the field current was provided by inserting a protective resistance (or, as it is called sometimes, a "discharge" resistance) immediately after removal of excitation supply, the time taken to slip the first pole was noticeably longer.

This effect is further accentuated when a rectifier (with negligible forward resistance) is connected across the field. Now, the time taken for the first pole to be slipped is four times longer than for the field open.

- 2) When the field was left open or was closed through a resistance, the induced field voltage is symmetrical (i.e. having half-cycles of equal duration). This voltage is mainly dependent on the magnitude of slip to which the machine settles down, and is of slip frequency.

In the case of simulated brushless scheme on the other hand, the magnitude of the induced inverse field voltage is proportional to the instantaneous value of slip (during the blocking period of rectifier) which itself varies considerably.

3) The fluctuations of the slip are relatively small for the field winding open or closed through a resistance. With a rectifier in the field circuit, the slip fluctuations are much more violent, and in fact it even changes sign after slipping of two successive poles. Briefly, this happens thus because in accordance with Lenz's Law when the rectifier is conducting, the induced field current tends to destroy its cause (i.e. the relative speed) by forcing a reduction of slip. When eventually the rectifier reaches its blocking state, the excitation torque component vanishes and the machine accelerates again.

4) In all the tests carried out it was found that the armature line current increases after removal of excitation (following a very brief initial transient effect). After this, for the field winding open or closed through a resistance, the armature current pulsations were gentle and relatively small. These

pulsations were considerably larger with the rectifier in the field circuit (see Subsections of 3.5).

Further tests have been made to investigate the effects of modifying some of the machine's parameters and inserting a discharge resistance in the field on its performance during asynchronous operation. These tests were only confined to the condition of field circuit closed through a rectifier.

It was found that:

- a. The peak inverse field voltage was considerably reduced by shunting the rectifier with a protective resistor.
- b. The magnitude of induced inverse voltage and slip remained almost constant when the quadrature-axis damping circuits were disconnected.
- c. Isolating 2/5 of the direct-axis damper bars caused the peak inverse voltage to increase by about 10%, and the machine's slip cycles to be of smaller period.
- d. When the damping winding was made completely inoperative the peak inverse voltage increased by about 25%, and the machine slipped more rapidly in comparison with other cases.

Apart from this extensive experimental programme, the performance of a.c. generator with rectifier in the field circuit was studied theoretically (see Chapter 2). It was shown that, the results obtained from the mathematical model used to analyse the asynchronous operation, correlate quite closely with the tested ones. The greatest discrepancy occurs in the prediction of performance for the quasi-steady asynchronous condition following the slipping of the first pole.

From the overall work carried out in the project, it can be stated that, the voltage grade of the diodes used in brushless machines will be determined not only by the maximum continuous rating (m.c.r.) excitation voltage, but also by the "ceiling excitation" condition corresponding to forcing of excitation by A.V.R. following sudden application of load, and by abnormal conditions. In the particular fault condition investigated here (asynchronous operation) a voltage of 3.5 times that at fractional steady load voltage prior to loss of excitation. Hence, if damage to the diodes is to be avoided, their ratings must be more than the magnitude of voltages induced during asynchronous operation. In practice, a bridge rectifier designed to withstand voltage of five times the rated excitation voltage can be considered as adequate.

In choosing this margin, attention must also be given to the voltage spikes which often occur when semiconductor diodes

are used in inductive circuits, particularly if direct switching is involved. These spikes can be easily suppressed by connecting a suitable voltage suppression network (RC) across the diodes. In this case only a capacitance was used.

For proper indication of the magnitude of such short duration spikes, a high quality cathode-ray tube must be used. The limited frequency response of u.v. recorder used no doubt attenuated the amplitude of the spikes recorded in Fig. 3.7(a) (the highest spike was lost in the photographing processing).

4.3 SUGGESTIONS FOR FURTHER WORK

The machine parameters used in theoretical computations were design parameters supplied by the manufacturer. It is felt that better results could have been obtained if test values of parameters were used instead. Test procedures suitable for determination of these parameters are described in Refs. 12 and 13.

The work presented in this project was concentrated only on the synchronous machine operating asynchronously in generating mode of small slip. The investigation could be extended to include the asynchronous operation of a synchronous motor with

brushless excitation scheme. In this case the voltage and current variations in the field circuit containing rectifiers during the whole starting process (for slips from 1.0 to 0) are inevitably much more severe. Now, the breaking torque due to unidirectional component of induced field current interferes with the starting performance and use of discharge resistor or additional thyristor in the field circuit becomes necessary. The effects of modifying the damping winding on the machine behaviour could then be studied.

TABLE 1 DESIGN PARAMETERS OF THE 69 kVA a.c. SYNCHRONOUS GENERATOR

Base armature voltage	415 V r.m.s. line
Base armature current	96 A r.m.s.
Base power	69 kVA
Base impedance	2.5 Ω
Base field voltage	6460 V
Base field current	5.34 A
Base field impedance	1210 Ω
Magnetising reactances:	
x_{md}	1.033 p.u.
x_{mq}	0.49 p.u.
Armature leakage reactance, x_a	0.061 p.u.
Armature resistance, r_a	0.015 p.u.
Field leakage reactance, x_f	0.167 p.u.
Field resistance, r_f	0.0021 p.u.
Damper leakage reactances:	
x_{kd}	0.042 p.u.
x_{kq}	0.016 p.u.
Damper resistances:	
r_{kd}	0.255 p.u.
r_{kq}	0.097 p.u.
Inertia constant, H	0.9 J/VA
<u>Calculated data</u>	
Transient reactance, x_d'	0.2049 p.u.
Subtransient reactances, x_d''	0.0936 p.u.
x_q''	0.0766 p.u.
Time constants, T_{do}'	1.8154 S
T_d'	0.3395 S
T_d''	0.0011 S
T_q''	0.0023 S

TABLE 2 DESIGN PARAMETERS OF THE 40 kVA TRANSFORMER

The following parameters of the transformer are referred to the bases of the armature circuit of 69 kVA a.c. generator.

Transformer reactance = 0.0411 p.u.

Transformer resistance = 0.0431 p.u.

APPENDIX A

RECTIFIER IN FORWARD BIAS

From equations (2.29) and (2.30) the derivatives of the flux linkages ψ_d and ψ_q are found as:

$$p\psi_d = \frac{x_d''}{\omega_o} \cdot pi_d + (x_d'' - x_a) \left[\frac{p\psi_f}{x_f} + \frac{p\psi_{kd}}{x_{kd}} \right] \dots\dots\dots(A.1)$$

and

$$p\psi_q = \frac{x_q''}{\omega_o} \cdot pi_q + (x_q'' - x_a) \frac{p\psi_{kq}}{x_{kq}} \dots\dots\dots(A.2)$$

Substituting for $p\psi_d$ (equation A.1) and ψ_q (equation 2.30) in the equation (2.4) of the axis voltage v_d , an expression which contains $p\psi_{kd}$ and $p\psi_f$ terms is obtained. The expressions for these are given in equation (2.31) and (2.33) respectively.

After rearranging the terms, an expression for pi_d is formed as:

$$pi_d = a_1 i_d + a_2 \omega i_q + a_3 \psi_f + a_4 \psi_{kd} + a_5 \omega \psi_{kq} + a_6 v_d + a_8 v_f \dots\dots\dots(A.3)$$

where $\omega = \omega_o - p\delta$.

δ is the load angle of the machine and is -ve for generator operation.

A similar expression is derived for pi_d .

The values of the constants $a_1, a_2 \dots$ etc. (of equation 2.34) are:

$$a_1 = - \left(r_a + \frac{x_{md} \cdot g_1^2}{g_3 \cdot \omega_o x_f T'_{do}} + \frac{g_1 \cdot g_2}{\omega_o x_{kd} \cdot T''_{do}} \right) \frac{\omega_o}{x''_d};$$

$$a_2 = - \frac{x''_q}{x''_d};$$

$$a_3 = \left(\frac{g_1}{x_f \cdot T'_{do}} + \frac{g_1 \cdot x_{md}^2}{x_f x_{kd} T'_{do}} - \frac{g_1 \cdot g_3}{x_{kd} x_f T''_{do}} \right) \frac{\omega_o}{x''_d};$$

$$a_4 = \left(\frac{g_1}{x_{kd} T''_{do}} - \frac{g_1 x_{md}^2}{g_3 x_f x_{kd} T'_{do}} \right) \frac{\omega_o}{x''_d};$$

$$a_5 = - \frac{g_2 \omega_o}{x_{kd} x''_d};$$

$$a_6 = \frac{\psi_o}{x''_d};$$

and $a_8 = - \frac{g_1 \omega_o}{x_f x''_d}$

where

$$g_1 = (x''_d - x_a)$$

$$g_2 = (x''_q - x_a)$$

$$g_3 = (x'_d - x_a)$$

Similarly it can be shown that:

$$b_1 = \frac{x''_d}{x''_q};$$

$$b_2 = - \left(r_a + \frac{g_2 x_{mq}}{\omega_o x_{kq} T''_{qo}} \right) \frac{\omega_o}{x''_q};$$

$$b_3 = \frac{\omega_o g_1}{x_f x''_q}; \quad b_4 = \frac{\omega_o g_1}{x_{kd} x''_q}; \quad b_5 = \frac{\omega_o g_2}{x_{kq} x''_q T''_{qo}}$$

$$b_6 = 0 ; \quad b_7 = \frac{\omega_0}{x_q''}$$

From equation (2.33) for $p\psi_f$:

$$c_1 = \frac{g_1 x_{md}}{\omega_0 g_3 T'_{do}} ; \quad c_3 = - \left[1 + \frac{g_1 x_{md}}{x_{kd} x_f} \right] \cdot \frac{1}{T'_{do}} ;$$

$$c_4 = \frac{g_1 x_{md}}{g_3 x_{kd} T'_{do}} ;$$

Similarly from equation (2.31) for $p\psi_{kd}$:

$$d_1 = \frac{g_3}{\omega_0 T''_{do}} ; \quad d_3 = \frac{g_3}{x_f T''_{do}} ; \quad d_4 = - \frac{1}{T''_{do}}$$

and from equation (2.32) for $p\psi_{kq}$:

$$e_2 = \frac{x_{mq}}{\omega_0 T''_{qo}} ; \quad e_5 = - \frac{1}{T''_{qo}}$$

APPENDIX B

RECTIFIER IN REVERSE BIAS

Differentiating the flux linkages in equations (2.38) and (2.39) with respect to time, it can be obtained that:

$$p\psi_d = \frac{x''_{dr}}{\omega_o} \cdot pi_d + (x''_{dr} - x_a) \frac{p\psi_{kd}}{x_{kd}} \dots\dots\dots(B.1)$$

$$p\psi_q = \frac{x''_q}{\omega_o} \cdot pi_q + (x''_a - x_a) \frac{p\psi_{kq}}{x_{kq}} \dots\dots\dots(B.2)$$

Substituting for $p\psi_d$ (equation B.1) and ψ_q (equation 2.39) in the equations (2.4) of the voltage v_d , an expression for $p\psi_{kd}$ is given in equation (2.35).

Rearranging the terms, pi_d can be expressed as:

$$pi_d = a_1^+ i_d + a_2^+ \omega i_q + a_4^+ \psi_{kd} + a_5^+ \omega \psi_{kq} + a_6^+ v_d \dots\dots(B.3)$$

A similar expression is derived for pi_q .

The values of the constants in equation (B.3) are:

$$a_1^+ = - \left(r_a + \frac{g_4 x_{md}}{\omega_o x_{kd} T'_{kdo}} \right) \frac{\omega_o}{x''_{dr}} ;$$

$$a_2^+ = - \frac{x''_q}{x''_{dr}} ; \quad a_4^+ = \frac{g_4}{x_{kd} T'_{kdo}} \cdot \frac{\omega_o}{x''_{dr}} ;$$

$$a_5^+ = - \frac{g_2}{x_{kq}} \cdot \frac{\omega_o}{x''_{dr}} ; \quad a_6^+ = \frac{\omega_o}{x''_{dr}}$$

where $g_4 = (x''_{dr} - x_a)$.

Similarly, from the expression for pi_d , it can be shown that:

$$b'_1 = \frac{x''_{dr}}{x''_q} ; \quad b'_2 = b_2 ; \quad b'_4 = \frac{x_{md}}{x_{md} + x_{kd}} \cdot \frac{\omega_o}{x''_q} ;$$

$$b'_5 = b_5 ; \quad b'_7 = b_7$$

From equation (2.35), for $p\psi_{kd}$:

$$d'_1 = \frac{x_{md}}{\omega_o T'_{kdo}} ; \quad d'_4 = - \frac{1}{T'_{kdo}}$$

Similarly from the equation (2.36) for $p\psi_{kq}$:

$$e'_2 = e_2 ; \quad e'_5 = e_5$$

Equation (2.37) can be written as:

$$p\psi_f = c_8 pi_d + c_9 p\psi_{kd}$$

where

$$c_8 = \frac{(x''_{dr} - x_a)}{\omega_o}$$

$$\text{and } c_9 = \frac{x_{md}}{x_{md} + x_{kd}}$$

Substituting for (pi_d) and $(p\psi_{kd})$ from equations (B.3) and

(2.35) in equation (2.37), the following expression is

obtained for $p\psi_f$:

$$p\psi_f = c_1' i_d + c_2' \omega i_q + c_4' \psi_{kd} + c_5' \omega \psi_{kq} + c_6' v_d$$

where:

$$c_1' = (a_1' c_8 + d_1' c_9)$$

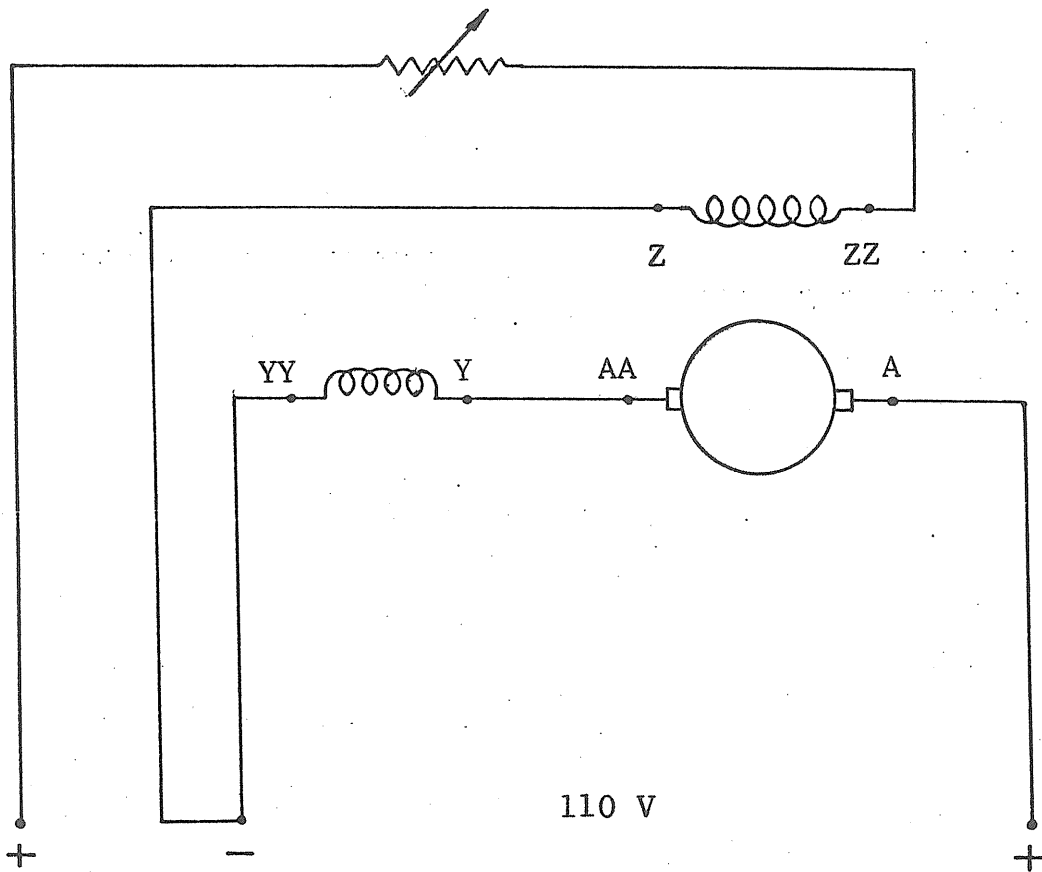
$$c_2' = c_8 a_2'$$

$$c_4' = (c_8 a_4' + c_9 d_4')$$

$$c_5' = c_8 a_5'$$

and $c_6' = c_8 a_6'$

APPENDIX C



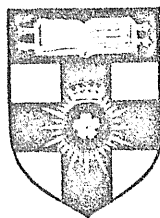
D.C. COMPOUND MOTOR SEPARATELY EXCITED

REFERENCES

1. Humphries, H.J. and Fairney, W.: 'Excitation rectifier schemes for large generators', Proc. I.E.E., Vol. 119, No. 6, June 1972, p. 661.
2. Horsley W.D.: 'Turbo-type generators', Proc. I.E.E., Vol. 110, No. 4, April 1963, p. 695.
3. Corbyn, D.B., Holburn, W.W. and Seydel, G.M.H.: 'Rectifier excitation for large turbo-alternators', Electrical Times, Dec. 1961, p. 837.
4. Panis, L.M.: 'Rectifier excitation of large turbo-generators', The Brown Boveri Review, MAR 1967, p. 69.
5. Easton, V.: 'Static rectifier excitation of large turbo-generators', G.E.C. Journal, Vol. 30, No. 1, 1963, p. 31.
6. Easton, V.: 'Excitation of large turbo-generators', Proc. I.E.E., Vol. 111, No. 5, May 1964, p. 1040.
7. Rao, K.V.N.: 'Fault studies on synchronous generators with rectifier excitation', Ph.D. Thesis, University of London, 1970.
8. Twardzicki, A. and Coleman, R.: 'Brushless salient-pole a.c. generators', Electrical Times, part 3, 1967, p. 610.
9. Adkins, B.: 'The general theory of electrical machines', (book) published by Chapman and Hall, 1959.
10. Alford, R.J.: 'The stability of a synchronous generator associated with an induction motor load', Ph.D. Thesis, University of London, 1964.
11. Mehta, D.B. and Adkins, B.: 'Transient torque and load angle of a synchronous generator following several types of system disturbance', Proc. I.E.E., 1960, 107A, p. 61.

12. Wright, S.H.: 'Determination of synchronous machine constants by test, reactances, resistances and time constants', Transactions A.I.E.E., December 1931, p. 1331.
13. I.E.C., Rotating electrical machines, Methods for determining synchronous machine quantities from tests, part 4, 1967, pp. 87.

UNIVERSITY OF LONDON



ROBERT ALEXANDER HANNA

of

QUEEN MARY COLLEGE

having completed an approved course of study in

ELECTRICAL MACHINES AND POWER SYSTEMS

as an Internal Student in the Faculty of ENGINEERING

and passed the prescribed examinations has this

day been admitted by the Senate to the degree of

MASTER OF SCIENCE

and awarded a Mark of Distinction

24 JANUARY 1974

B. A. Phillips

Vice-Chancellor